South-Central Barents Sea Composite Tectono-Sedimentary Element

A. G. Doré[1]*, T. Dahlgren[2], M. J. Flowerdew[3], T. Forthun[2], J. O. Hansen[2], L. B. Henriksen[2], K. Kåsli[2], B. Rafaelsen[2], A. E. Ryseth[2], K. Rønning[2], D. Similox-Tohon[2], A. Stoupakova[4] and O. Thießen[2]

[1]Energy & Geoscience Institute (EGI), London, 423 Wakara Way, Suite 300, Salt Lake City, UT 84108, USA (based in London)

[2]Equinor ASA, PO Box 40, Harstad, Norway

[3]Cambridge Arctic Shelf Programme (CASP), West Building, Madingley Rise, Madingley Road, Cambridge CB3 0UD, UK

[4]Lomonosov Moscow State University, GSP-1, Leninskie Gory, Moscow, 119991, Russia

TD, 0000-0002-1766-3041; MJF, 0000-0002-9710-2593; JOH, 0000-0001-7828-1066; LBH, 0000-0002-9390-2358; OT, 0000-0002-5689-4117
*Correspondence: agdore@gmail.com

Abstract: The south-central Barents Sea today comprises a shallow continental shelf with water depths mainly in the 200–400 m range, straddling the Norway–Russia marine boundary. Geologically, it consists of a stable platform (the Bjarmeland Platform) dissected by rifts of probable Late Carboniferous age, with a significant and geologically persistent basement high (the Fedynsky High) in its southeastern part. The rifts are the ENE–WSW-trending Nordkapp Basin, the similarly trending but less clearly demarcated Ottar Basin and the NW–SE Tiddlybanken Basin. The varying rift trends appear to reflect the orogenic grain patchwork of the basement (Caledonide and Timanide), and these basins were infilled with a variable facies assemblage including substantial Carboniferous–Permian halites.

A massive sedimentary influx of fluvio-deltaic to shallow-marine sediments took place in the Triassic, from the east and SE (Urals, Novaya Zemlya and western Siberia) and the south (Baltic Shield), resulting in doming and diapirism in the areas of thickest salt, particularly in the rifts. The succeeding Jurassic, Cretaceous and Cenozoic successions are generally thin, locally thickening in rim synclines and in the NE of the area towards the deep basins flanking Novaya Zemlya. Reactivation of the halokinetic structures took place in the early Cenozoic, probably associated with the development of the NE Atlantic–Arctic Ocean linkage.

Marine source rocks of Triassic and Late Jurassic age are present in the area, along with Carboniferous and Permian source rocks of uncertain effectiveness. Petroleum has been found in Jurassic and Triassic clastic reservoirs, including recent shallow Jurassic oil and gas discoveries. Although none is currently in production, near-future oil development is likely in the Wisting discovery, on the western margin of the area. New exploration, including drilling, has taken place in the east of the area as a result of recent Norwegian and Russian licensing.

The shallow continental shelf of the south-central Barents Sea is shown in its Arctic context in Enclosures A and E of this volume, and more locally in Figure 1. Following the terminology used in this Memoir, it is described as a Composite Tectono-Sedimentary element (CTSE) because although it includes rifts (Nordkapp and Tiddlybanken basins), basement-controlled highs (Fedynsky High) and a platform (Bjarmeland Platform), these elements were unified as a single broad, intercratonic basin in the Triassic–Middle Jurassic. Bordering TSEs described in this Memoir include the northern Barents Sea (Lundschien *et al.* 2021), the East Barents (Drachev *et al.* 2021), the Finnmark Platform to the south (Henriksen *et al.* 2021*b*), and the Hammerfest Basin and Loppa High to the west (Brunstad and Rønnevik 2021; Henriksen *et al.* 2021*a*).

The area is sparsely explored but does include a number of petroleum discoveries, most of which are currently considered uncommercial. Minor gas and oil accumulations (the Nucula, Bamse and Binne fields) have been discovered in the southwestern Nordkapp Basin, and a modest-sized gas field has been found on the Norsel High on the NW flank of the Nordkapp Basin. On the Bjarmeland Platform, Wisting and Hanssen are promising Jurassic oil discoveries at shallow depth, while all other discoveries to date on the platform are gas. They include the Norvarg, Ververis and Arenaria accumulations, and a complex of shallow Jurassic gas reservoirs including the Intrepid Eagle and Atlantis discoveries. Several large gas discoveries have been made in the Russian sector to the east of the study area. These include Ludlovskoe, Shtokman, Severo-Kildinskoe and Murmanskoe.

A treaty between Russia and Norway on maritime delimitation and collaboration in the Barents Sea and the Arctic Ocean came into force on 7 July 2011, and shortly afterwards a process began in both international sectors to open this part of the Barents Sea for petroleum activities. At the time of writing, extensive leasing has occurred in the Russian part of the formerly disputed zone, while licensing of parts of the eastern Norwegian Barents Sea in the Norwegian 23rd Licensing Round has given rise to new drilling results.

Age

The principal basin fill of the area is Late Paleozoic (Carboniferous)–Triassic, with a thinner Jurassic and partially eroded Cretaceous cover. Paleogene–Neogene rocks are thin or absent over most of the area, while a thin but persistent layer of Quaternary glaciomarine sediments forms the seabed. The Cenozoic–Quaternary configuration is largely the result of late uplift and erosion, which removed up to 1500 m of the younger sedimentary cover (e.g. Henriksen *et al.* 2011*a*). Cretaceous rocks subcrop to the Quaternary over most of the south-central Barents Sea, except where diapiric Carboniferous–Permian halites break through the Cretaceous cover in the axes of the Nordkapp and Tiddlybanken basins and in the Svalis Dome, and where Triassic rocks emerge in the core of a major palaeohigh, the Fedynsky High.

Geographical location and dimensions

The south-central Barents Sea comprises approximately 150 000 km^2 of continental shelf, located 50–200 km off the northern coast of Norway and the bordering Russian coast (Enclosure A). The eastern part of the CTSE oversteps the median line between the Norwegian and Russian territorial waters. The entire area is a part of a shallow-marine shelf, with water depths of the order of 200–400 m (Fig. 1).

From: Drachev, S. S., Brekke, H., Henriksen, E. and Moore, T. (eds) *Sedimentary Successions of the Arctic Region and Their Hydrocarbon Prospectivity*. Geological Society, London, Memoirs, **57**,
https://doi.org/10.1144/M57-2017-42

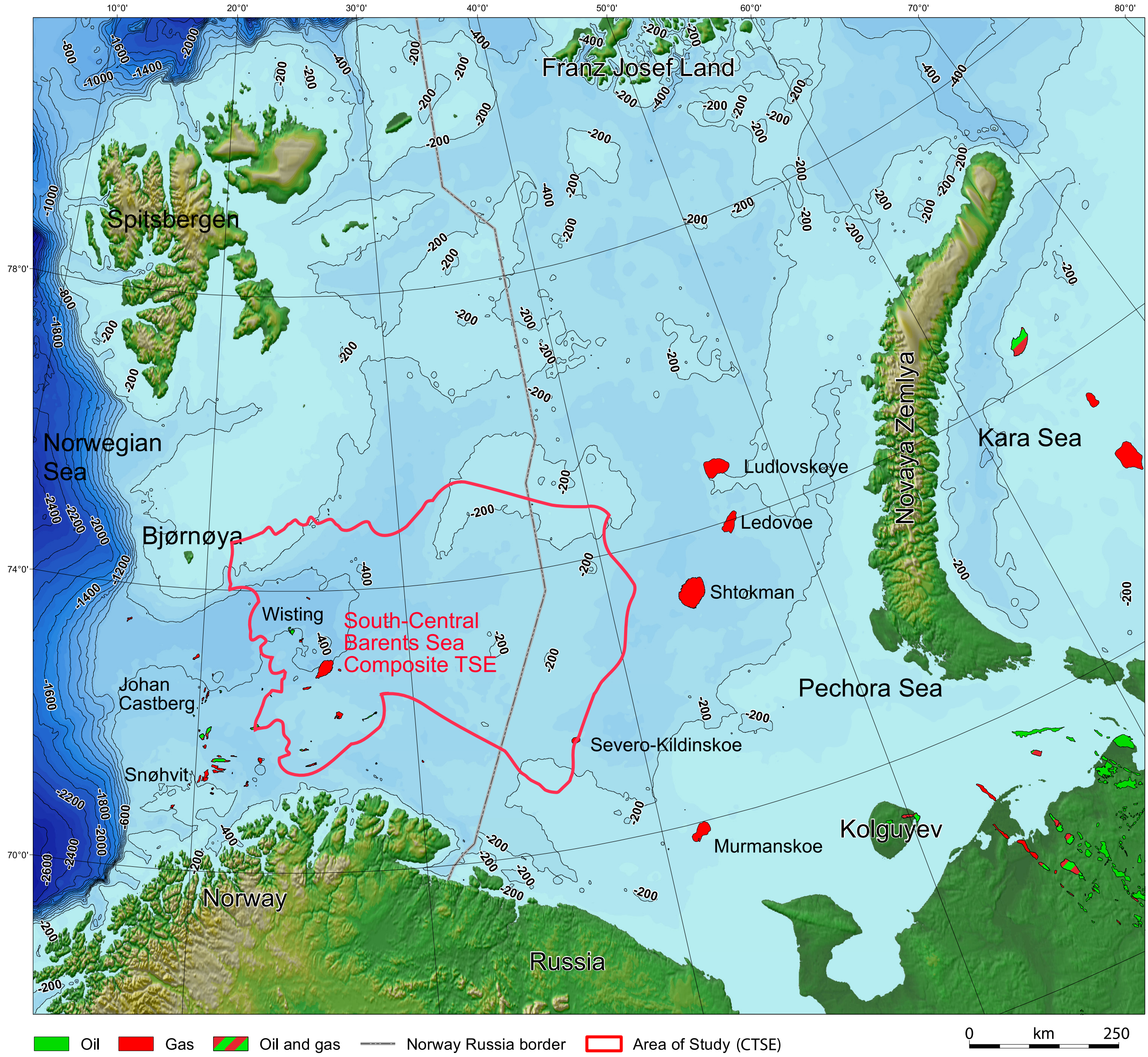

Fig. 1. Barents Sea bathymetry and location of the South-Central Barents Sea CTSE.

Principal datasets

Offshore wells and key regional seismic lines over the CTSE are shown in Figures 2 and 3, and in Enclosure F of this volume.

Wells

Selected exploration wells and key discoveries in the area are shown in Figure 2. The area is sparsely drilled in both the Norwegian and Russian sectors. The area was targeted by about 20 IKU (Continental Shelf Institute, now SINTEF Petroleum Research) shallow stratigraphic boreholes in 1987–88, which provided a useful early indicator of the region's stratigraphy (see Bugge *et al.* 2002, for a synopsis of the key results). On the Norway side, 7226/11-1 was drilled on the Norsel High in 1987, and currently some 15 industry wildcat wells have been completed in, or on the margins of, the Nordkapp Basin. At the time of writing, a similar number of exploration wells have been drilled on the Bjarmeland Platform; activity is highest on the western margin of the area, where, for example, five appraisal wells have been drilled on the Wisting oil discovery. Recent drilling in the NE of the study area (well 7435/12-1) resulted in the Korpfjell gas discovery.

The Russian side consists of the western flank of the East Barents megabasin system, and is also sparsely drilled. However, a short distance to the east lie significant drilled hydrocarbon accumulations (mainly gas) such as Severo-Kildinskoe, Shtokman and Ludlovskoe, which provide important stratigraphic control. Drilling of this area started slightly earlier than the Norwegian drilling (Severo-Kildinskoe in 1983, Murmanskoe in 1985 and Shtokman in 1988).

Seismic data

The area is covered by 2D seismic of variable density, with higher densities in the more explored axis of the Nordkapp Basin and in the Wisting–Intrepid Eagle area to the NW, and looser grid data in the border zone between Norway and Russia. 2D seismic in the Norway sector adjacent to the median line with Russia, originally obtained by the Norwegian Petroleum Directorate (NPD), was reprocessed in 2013–15 as a precursor to the Norwegian 23rd Licensing Round. Local 3D high-quality datasets exist in the Nordkapp Basin and in the

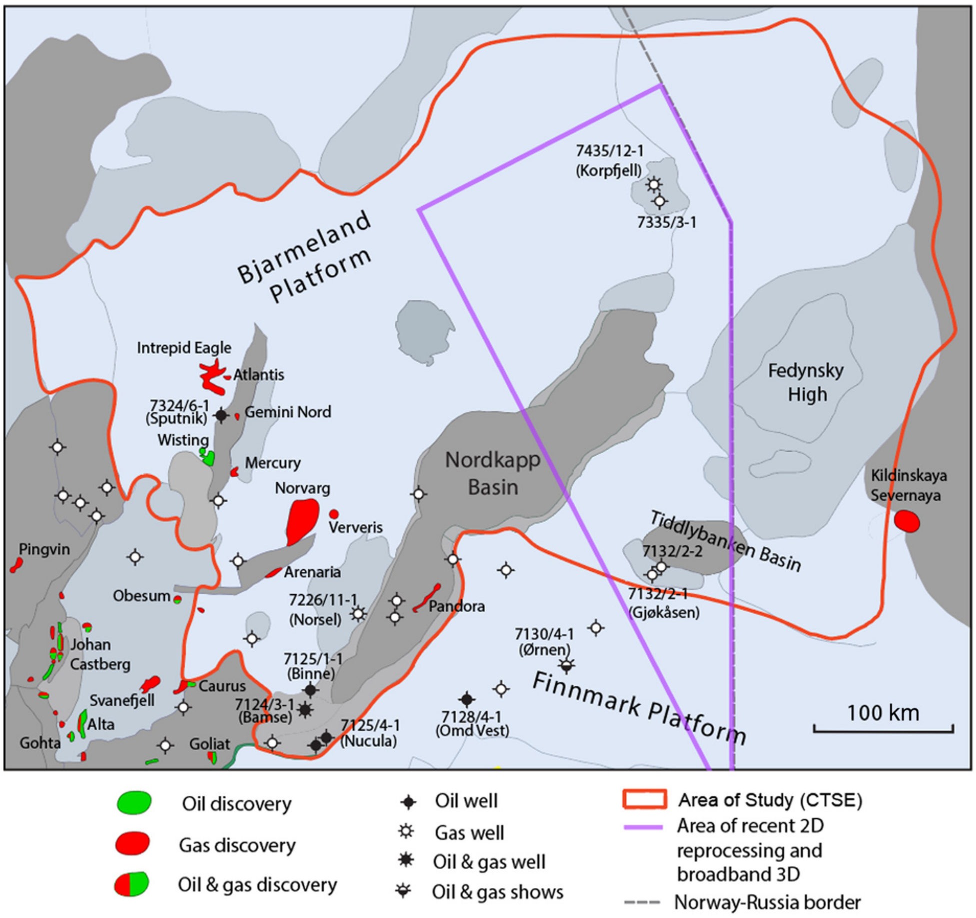

Fig. 2. Location of discoveries and selected wells described in this paper. Where the outlines of discoveries are indicated, discovery and appraisal wells are not shown. The purple outline shows the area of intensive 2D seismic reprocessing and 3D broadband seismic acquisition, associated with the Norwegian 23rd Licensing Round. Structural elements from Figure 3 are shown in greyscale for reference.

western part of the CTSE, the most recent being in the Wisting–Intrepid Eagle area. Four broadband 3D surveys were acquired in 2014 close to the Russian border in a group shoot, also in support of the 23rd Round (Fig. 2).

Other data

The entire area is covered by aeromagnetic data of various vintages, including a new (39 000 km^2) dataset acquired by the Norwegian Geological Survey (NGU). Likewise, gravity data are available across the whole area, incorporating satellite gravimetric data, gravity stations on mainland Norway, and marine gravity data from commercial companies, universities, the NPD and the NGU. Enclosures B and C of this volume show gravity and magnetic maps of the CTSE in a full Arctic context.

Controlled source electromagnetic (CSEM) data have been obtained by Equinor in the NW of the study area, and in the SE with particular focus on the areas covered by the recent broadband 3D seismic. Older vintage CSEM surveys also exist in the Nordkapp Basin.

Tectonic setting, boundaries and main tectonic/erosional/depositional phases

The South-Central Barents Sea CTSE can be described as a series of Late Paleozoic evaporite-bearing rift basins (e.g. the Nordkapp and Tiddlybanken basins) overprinted by a broad intracratonic sag basin of Triassic age, and further modified by halokinesis, extension and inversion (Figs 3 and 4). It is bounded to the north by two palaeohighs of probable Mesozoic origin: the Gardarbanken and Sentralbanken highs. Its western margin is formed (from south to north) by the transition between the Nordkapp and Hammerfest basins, by a large Paleozoic palaeohigh (the Loppa High) and a Mesozoic ramp (the Fingerdjupet Sub-basin) flanking the Bjørnøya Basin. To the south lies the Finnmark Platform, rising up onto the Norwegian mainland (Henriksen *et al.* 2021*b*), and to the east lies the South Barents Basin (Drachev *et al.* 2021), part of the giant Russian Barents Sea megabasin complex flanking Novaya Zemlya (see Enclosure A; also Gabrielsen *et al.* 1990; Henriksen *et al.* 2011*b*).

The south-central Barents Sea area has uniformly thick crystalline crust, significantly thinner than Baltica. Basement thicknesses of between 20 and 25 km are recorded outside of the Nordkapp Basin, beneath which slightly lower thicknesses are recorded (Klitzke *et al.* 2015). Its substructure reflects the intersection of several major orogenic belts: Timanian, Caledonian and Uralian (Fig. 5 and Enclosure D of this volume).

The Timanian basement assemblage is marked by the WNW–ESE trend of the Trollfjord–Komagelv Fault and SW-verging folds on the Varanger and Kola peninsulas (Roberts and Siedlecka 2002), and is apparently reactivated in the trend of the Tiddlybanken Basin (Shulgin *et al.* 2018). The Timanides represent a Late Neoproterozoic (630–540 Ma) accretionary orogen along the northeastern margin of Baltica (e.g. Gee and Pease 2004).

The Silurian Caledonian Orogeny (Scandian Orogeny) records closure of the Iapetus Ocean and continent–continent collision with the fusing of Baltica with Laurentia between 431 and 428 Ma (Kirkland *et al.* 2006). The precise position of both the Caledonian (Iapetus) suture and the Caledonian deformation front in the Barents Sea is obscured by the thick sedimentary blanket, and has been a matter of debate. While the Iapetus suture very probably traverses the west of the study area (Gee and Teben'kov 2004: Aarseth *et al.* 2017), modern aeromagnetic surveys (Fig. 6) (e.g. Gernigon

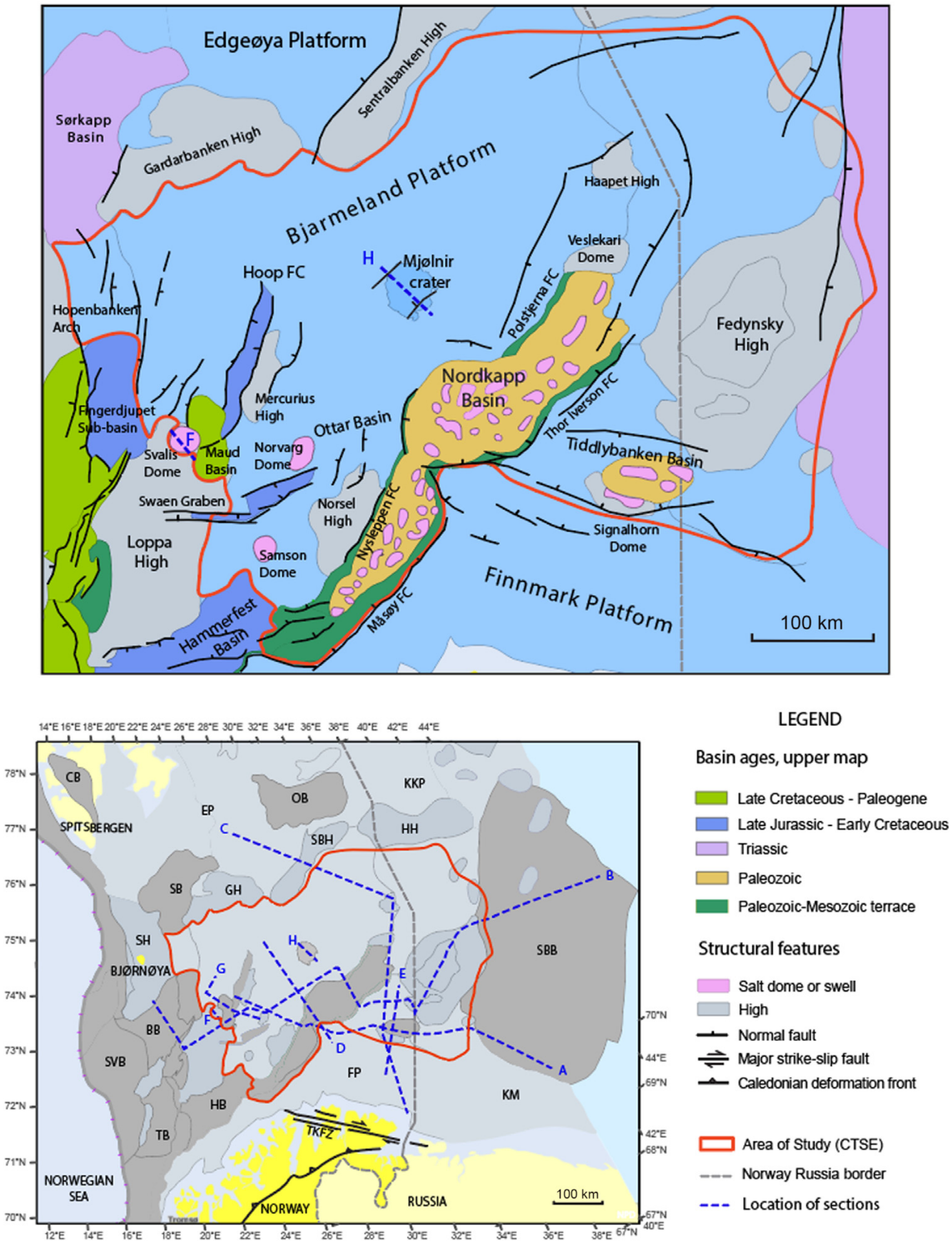

Fig. 3. Structural features, basin ages (upper map) and setting (lower map) of the South-Central Barents Sea CTSE. Locations of seismic and geoseismic sections in later figures are shown in blue. Abbreviations: BB, Bjørnøya Basin; CB, Central Basin of Spitsbergen; EP, Edgeøya Platform; FP, Finnmark Platform; GH, Gardarbanken High; HB, Hammerfest Basin; HH, Hopen High; KKP, Kong Karl Platform; KM, Kola Monocline; OB, Olga Basin; SB, Sørkapp Basin; SBB, South Barents Basin; SBH, Sentralbanken High; SH, Stappen High; SVB, Sørvestnaget Basin; TB, Tromsø Basin; TKFZ, Trollfjord–Komagelv Fault Zone.

et al. 2014) suggest that the Caledonian nappes swing anticlockwise from an initial NE–SW trend in the southern part of the Finnmark Platform to NNW–SSE across the Nordkapp Basin and into the Bjarmeland Platform (Fig. 5).

The Uralian orogenic belt was formed by episodes of arc and continental accretion to the Baltican margin, which began in the Carboniferous and culminated during the Permian. Novaya Zemlya forms part of the Arctic extension of the orogen. Movements in Novaya Zemlya were later than the main Uralian events, with folding at the end of the Triassic (Zhang *et al.* 2018) and some minor tectonic activity persisting as late as the Late Cretaceous (Stoupakova *et al.* 2011). Post-orogenic subsidence on the margins of the CTSE, in the South Barents Basin, appears to be isostatically compensated, as evidenced by a bland response on the Bouguer gravity map (Fig. 6).

The Late Paleozoic age of rifting is based on seismic observations, ties to shallow cores on the Finnmark Platform (Bugge *et al.* 2002), on assumed equivalence of the infilling halites to the evaporitic Gipsdalen Group of Svalbard (e.g. Dallmann 1999) and on observations of Late Paleozoic tectonics on Svalbard (Braathen *et al.* 2011). The thick halites of the Nordkapp Basin imply that a substantial fault-generated depression developed during the Late Paleozoic (probably Middle–Late Carboniferous: e.g. Gudlaugsson *et al.* 1998). Not all of this thickness corresponds to fault-defined relief, however, because salt was also deposited in the basin during the subsequent phase of differential thermal subsidence.

Following the rifting, the Uralian collision and suturing between Baltica and Siberia at the Permian–Triassic transition resulted in a major change of tectono-sedimentary regime. A thick Permo-Triassic continental–marine succession prograded from easterly and southeasterly provenances – the Uralian–Novaya Zemlya fold belt and the area occupied by the present-day South Kara and West Siberian basins – and, to a lesser extent, from the Baltic mainland in the south (e.g. Glørstad-Clark *et al.* 2011; Henriksen *et al.* 2011*b*; Eide *et al.* 2017). The Triassic succession alone reaches 6 km in thickness immediately east of the area in the South Barents Basin, with the lowermost Triassic unit, the Havert Formation and equivalents, accounting for more than half the total thickness. Triassic loading, perhaps enhanced by compressive push

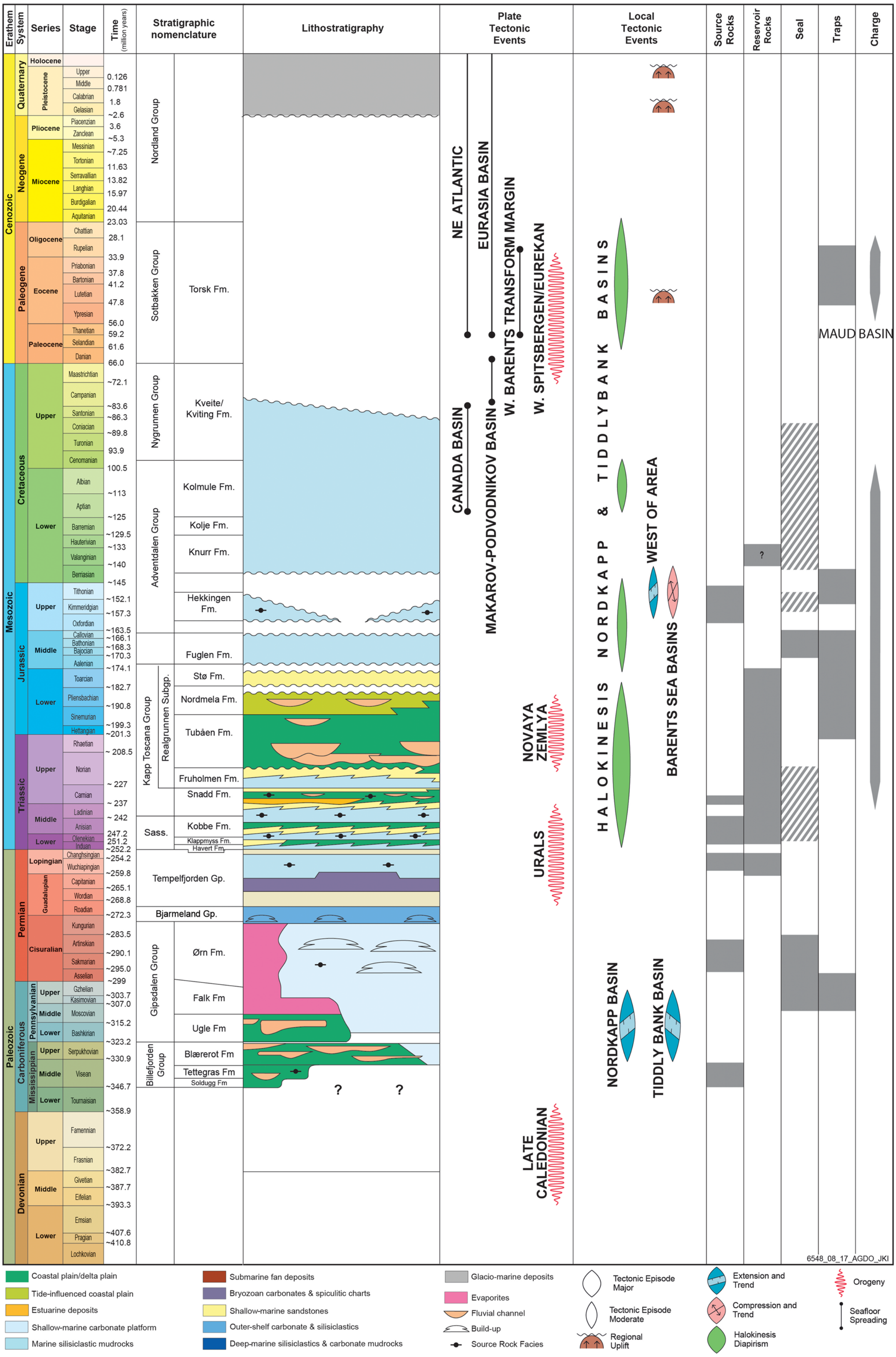

Fig. 4. Tectonostratigraphic chart for the south-central Barents Sea. Petroleum system elements (source, reservoir, seal, trap and charge) are shown to the right.

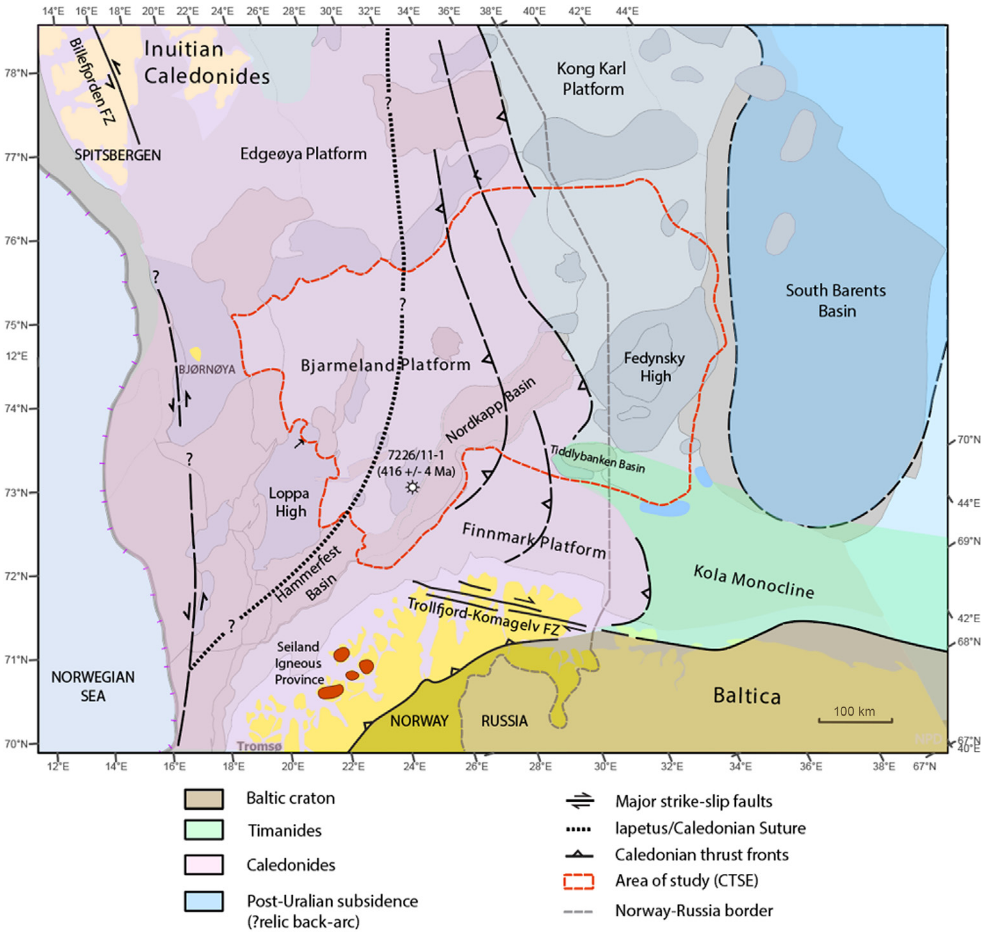

Fig. 5. Principal basement terranes and orogenic trends in and around the Barents Sea. The conjectural Caledonian nappe trend across the TSE essentially follows the concept of Gernigon *et al.* (2014). Younger basin outlines from Figure 2 are shown for reference.

from the developing Uralides, induced halokinesis (pillows, domes and canopies) in the Nordkapp and Tiddlybanken basins, and some milder halokinetic phenomena (domes and swells) outside of the main basins (Fig. 3). A difference in timing of the main halokinesis is observed between the Nordkapp Basin (Early–Middle Triassic) and the Tiddlybanken Basin (Middle–Late Triassic). The later phase of diapirism in the Tiddlybanken Basin may be due to smaller thicknesses of salt, which only became mobile with higher sediment loads. In general, halokinetic activity diminishes eastwards into the Russian sector, with occasional salt pillowing observed between the palaeohighs. The most logical explanation for this reduction is that this area represents the eastern limit of the late Paleozoic rift network, and hence of the thick salt. Although the most intense halokinetic movements were of Triassic age, some activity persisted through to the Cenozoic, particularly at the western margin of the area. Rejuvenation of salt movement was episodic, and was triggered by far-field effects of rifting and compression.

In the Late Jurassic and Early Cretaceous, significant rifting took place to the west of the study area, in the Hammerfest Basin and on the western Barents margin (e.g. Gabrielsen *et al.* 1990; Ryseth *et al.* 2021). In the study area, this extensional faulting is best expressed in the vicinity of the Nucula Field, in the Nysleppen Fault Complex at the Nordkapp Basin–Hammerfest Basin transition, and in the Hoop Fault Complex (Fig. 3). This episode is largely unobserved farther east in the study area. Rather, transitioning eastwards, a change to a mildly compressive (or transpressive) regime is observed. This is indicated by the formation of domal structures in the South Barents Basin such as Shtokman and Severo-Kildinskoe, and by thickness relationships observed on new seismic, demonstrating rejuvenation of the Fedynsky High. The domes in the Russian sector often have a NE–SW orientation, and the origin of this grain is poorly understood. It is possible that the domes bear more relation to the kinematics of the opening of the Arctic Ocean to the north (e.g. Lawver *et al.* 2002; Doré *et al.* 2015) and to late stage movements in the Novaya Zemlya fold belt, rather than events to the west.

In the latest Cretaceous and Cenozoic, episodic inversion, uplift and exhumation affected the area (Fig. 4). The first of these events, probably peaking in the Eocene, was a reflection of both the opening of the NE Atlantic Ocean to the west (e.g. Faleide *et al.* 2010) and the Eurasia Basin of the Arctic Ocean to the north (e.g. Doré *et al.* 2015). A transform linkage between the two oceans occurred along the western Barents Sea margin, with significant associated transpression and transtension, causing far-field effects in the study area. A new phase of salt diapirism, triggered by compression rather than sedimentation, took place in the Nordkapp Basin and in salt-cored domes to the west on the Bjarmeland Platform such as Norvarg, Ververis, Samson and Svalis. Folding of Cretaceous strata in the Haapet Dome (Fig. 3) can also be attributed to this episode, as can a late phase of development of the large inversion domes in the Russian Barents Sea basins, although timing there is poorly constrained due to the removal of the sedimentary overburden. Some late rejuvenation of normal faults also took place in the Nordkapp Basin.

The uplifted and eroded nature of the Barents Sea is well known (e.g. Nyland *et al.* 1992; Henriksen *et al.* 2011*a*). While numerous uplifts of basins and highs within the province took place through the Paleozoic and Mesozoic as a result of inversion, block faulting and halokinesis, the most pervasive regional uplifts undoubtedly took place during the Cenozoic. Although the south-central area underwent less erosion than some other parts of the Barents Sea, the net erosion was still significant and is placed at around 1500 m by most authorities (e.g. Henriksen *et al.* 2011*a*; Ktenas *et al.* 2017).

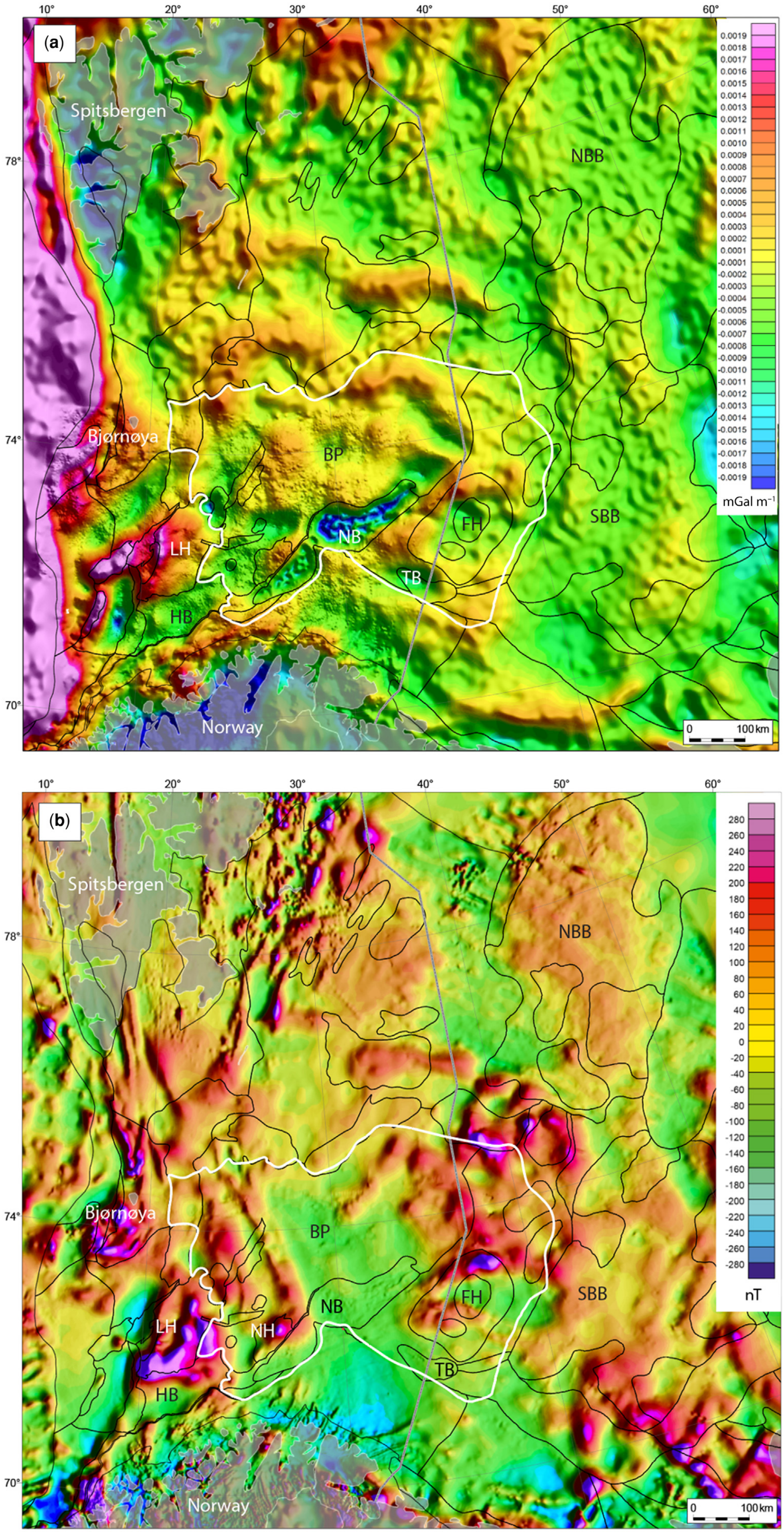

Fig. 6. Gravity and magnetic maps of the Barents Sea, showing the TSE location and setting. (a) Bouguer gravity map. (b) Total intensity magnetic map. Basin outlines are shown for reference. Abbreviations: BP, Bjarmeland Platform; HB, Hammerfest Basin; FH, Fedynsky High; LH, Loppa High; NB, Nordkapp Basin; SBB, South Barents Basin; TB, Tiddlybanken Basin.

Basin modelling, including apatite fission-track analysis (AFTA), indicates two main regional events. The first was of approximately Eocene age, most probably associated with the Atlantic margin break-up and inversion described above. As a result, Cenozoic sedimentation was sparse in the south-central Barents Sea and the pre-existing Cretaceous cover was partially eroded. The second erosional episode, which again affected the entire Barents Sea, was of Pliocene-Pleistocene age, and was associated with repeated erosion and isostatic uplift during the northern hemisphere glaciations. The erosional signature of this event is the Upper Regional Unconformity (URU), which truncates strata of Late Paleozoic–Cenozoic age in the area, and is overlain by thin Quaternary glacio-marine deposits.

The structural development of the south-central Barents Sea is interesting in a broader context, as part of the evolution of a major cratonic basin. Outside of the massive subsidence alongside the eastern margin of Novaya Zemlya, and the halokinetically-influenced sequences of the rift basins, the platform areas still accumulated substantial thicknesses of sediments, particularly in the Triassic. This depositional area was part of a much wider entity encompassing the greater Barents Sea, Svalbard and Arctic Canada (Sømme *et al.* 2018). Although periodically marine, this broad area of subsidence was internal to the Pangaean supercontinent and separated from the nearest true ocean, the palaeo-Pacific margin. As with other major cratonic basins such as the West Siberian Basin to the SE, the genesis of this continental-scale subsidence is poorly understood and is a fertile area for future study. For some current ideas on cratonic basin formation, see Allen and Allen (2013) and McKenzie and Priestley (2016).

Underlying and overlying rock assemblages

Age of underlying basement or youngest underlying sedimentary unit

Orogenic belts and postulated basement substructure of the CTSE and surrounding area are shown in Figure 5, and in their wider context in Enclosure D. Pre-Upper Paleozoic basement penetrations are rare but, by comparison with the adjacent Norwegian mainland and nearby Russian mainland (e.g. Ramberg *et al.* 2006), may consist of Precambrian Baltic-Shield-type basement, ranging in age from the Archean to Neoproterozoic, and early Paleozoic–Devonian tectonic assemblages from the Caledonian Orogeny. A single basement core in well 7226/11-1 on the Norsel High provides local confirmation of the latter rock suite. The basement at this location consisted of a kyanite-bearing biotite schist (e.g. Slagstad *et al.* 2008). Rb–Sr dating of the sample by one of us (MJF) has yielded a biotite mineral age of 416 ± 4 Ma, consistent with cooling following Caledonian (Scandian) deformation and metamorphism. However, no zircons for U/Pb dating were retrieved from the core, and thus, to date, it has not been possible to determine the depositional age of the metasediments (Pascal *et al.* 2010).

A marked positive magnetic anomaly on the Norsel High (Fig. 6) is unlikely to relate to the rock type found in the 7226/11-1 core, and may indicate deeper igneous rocks akin to the Neoproterozoic Seiland Igneous Province of northern Norway (Fig. 5) (e.g. Pastore *et al.* 2018).

Age of oldest overlying sedimentary unit

A thin veneer of Pleistocene-Recent glaciomarine and shallow-marine sediments is present over the area. This overlies the URU, which represents a significant episode of Plio-Pleistocene glacial and periglacial erosion. These superficial sediments are not included in the CTSE, and thus constitute the oldest overlying sedimentary unit.

Subdivision and internal structure

Structurally, the south-central Barents Sea comprises a moderately deformed subsiding platform traversed by Late Paleozoic rifts (the Nordkapp and Tiddlybanken basins and the less well-demarcated Ottar Basin) (Fig. 3, cross-sections of Figs 7–9 and Enclosure E). It has been strongly loaded by a thick Permo-Triassic continental–marine succession prograding from the Uralian–Novaya Zemlya fold belt in the east and, to a lesser extent, the Baltic mainland in the south (e.g. Glørstad-Clark *et al.* 2011; Henriksen *et al.* 2011*b*; Eide *et al.* 2017).

Late Carboniferous–Permian salt is widespread over the area but is thickest in the rifts, the positions of which are marked by intense halokinetic activity. The thick salt and associated doming are well resolved as major lows on the Bouguer gravity map of Figure 6. The two rifts trend almost orthogonally to each other, and clearly reflect exploitation of older tectonic grain (Fig. 5). The Nordkapp Basin, like the en echelon Hammerfest Basin to the west, reflects the NE–SW (Silurian–Devonian) Caledonian orogenic trend of the adjacent Norwegian mainland. Notably, however, the Carboniferous–Permian development of the two basins was different, and the Hammerfest Basin does not have a thick salt succession. The Tiddlybanken Basin mimics the NW–SE late Precambrian Timanian (Baikalian) orogenic trend of the Kola Peninsula and the Timan–Pechora Basin in NW Russia. The interplay between these two trends is further illustrated by the offset between the Hammerfest and Nordkapp basins, probably occurring where the basins are intersected by the offshore projection of the NW–SE Trollfjord–Komagelv Fault (e.g. Gabrielsen and Færseth 1989) (Figs 3 and 5). The structural geometries suggest that this major dextral transcurrent fault of late Precambrian–Ordovician age was probably utilized as a transfer zone by the Late Paleozoic basins, although this interpretation has been disputed by Koehl *et al.* (2018).

The Nordkapp Basin can be divided into three main segments: SW, central and NE. The southwestern segment displays a marked asymmetrical cross-section (e.g. Figs 7 and 10). The main displacement occurred along the Nysleppen Fault Complex bordering the basin to the NW, creating a half-graben. The central segment has a more east–west-orientated basin axis and is much deeper, without clear half-graben geometry at depth. Equinor estimates of the amount of salt deposited in the basin, carried out by flattening on a near Base Permian horizon, show that the central segment contains the thickest salt section of the Nordkapp Basin. The NE segment is again orientated more northeasterly and displays an opposite half-graben polarity compared to the SW segment, as the continuation of Thor Iversen Fault Complex bounding the basin to the SE takes up most of the displacement (e.g. Figs 8 and 9).

The southern flank of the Nordkapp Basin is formed by the Finnmark Platform, characterized by a generally simple, monoclinal dip towards the basin. Like the Bjarmeland Platform, it has a thick blanket of late Paleozoic and Triassic sediments, which truncate towards the Norwegian mainland. It is described by Henriksen *et al.* (2021*b*)). The Finnmark Platform merges eastwards into the NW–SE Kola Monocline (Drachev *et al.* 2021), which parallels and arguably defines the coast of the Russian Kola Peninsula. Running parallel to the monoclinal strike and the peninsula, the Tiddlybanken Basin shows evidence of half-graben geometries on both

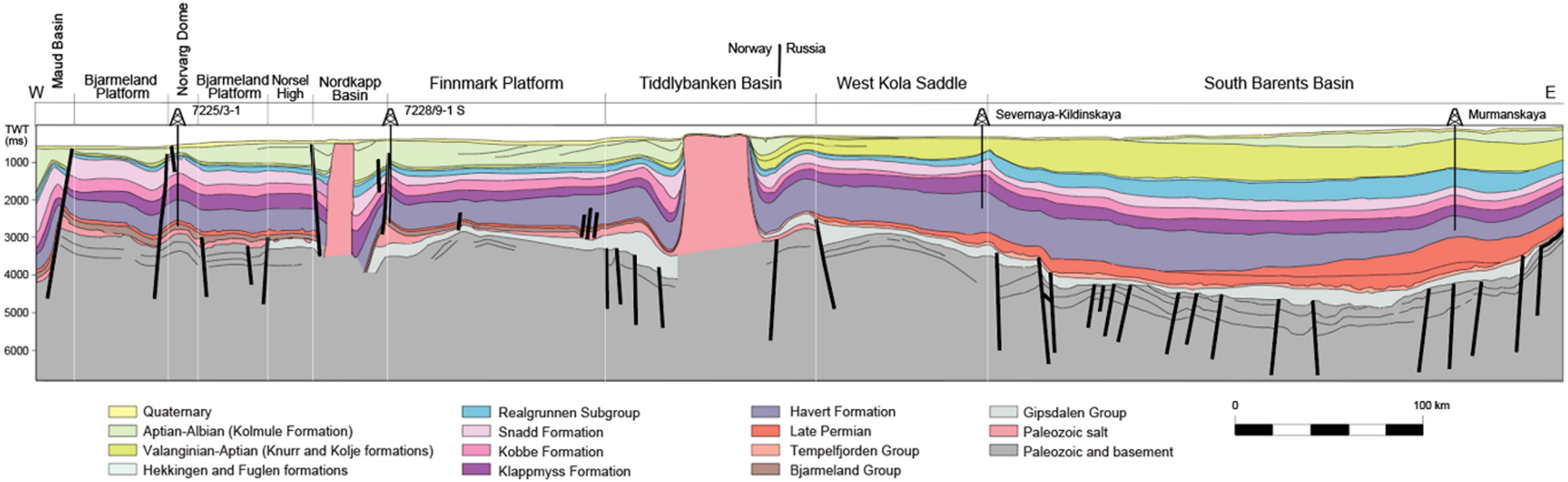

Fig. 7. West–east super-regional geoseismic profile (line A in Fig. 3) crossing the Bjarmeland Platform, Nordkapp Basin, Finnmark Platform, Tiddlybanken Basin and South Barents Basin.

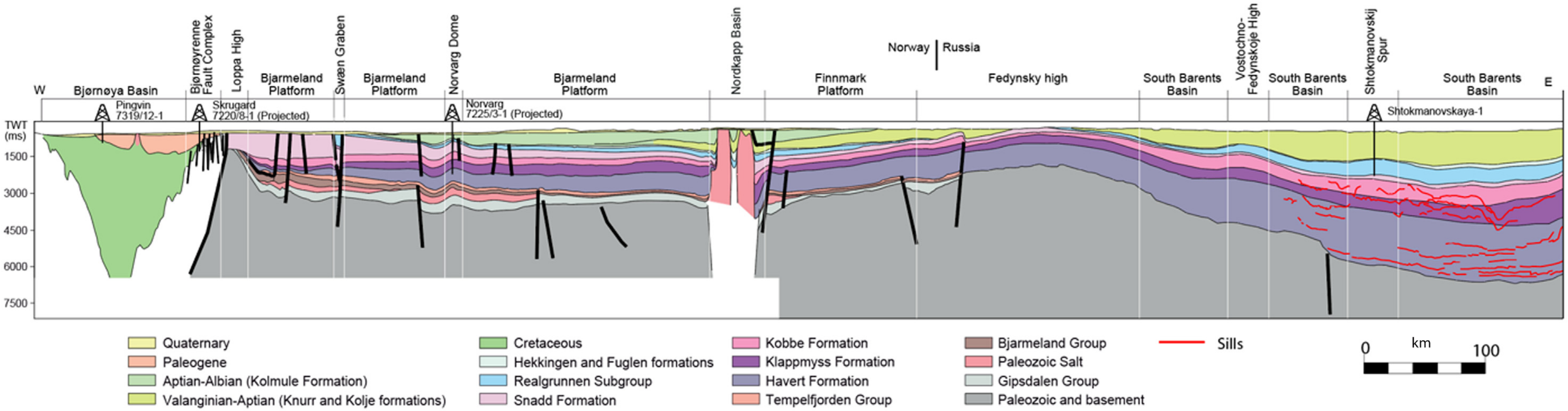

Fig. 8. West–east super-regional geoseismic profile (line B in Fig. 3) crossing the Bjarmeland Platform, Nordkapp Basin, Finnmark Platform, Fedynsky High and South Barents Sea Basin.

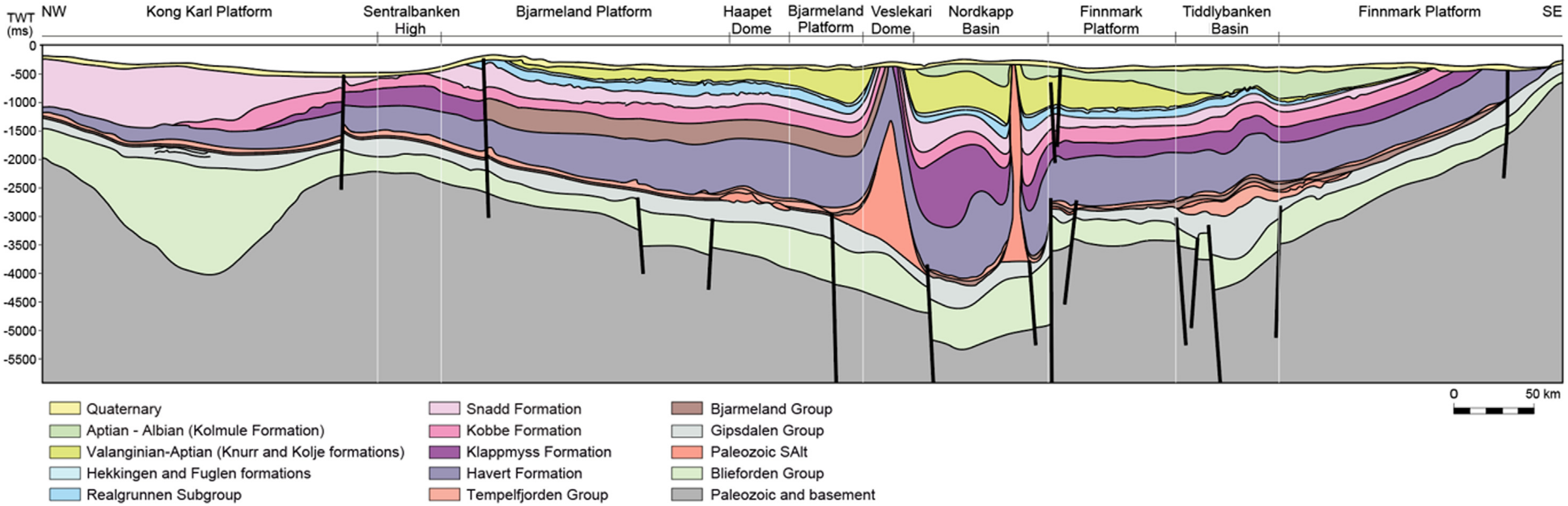

Fig. 9. NW–SE super-regional geoseismic profile (line C in Fig. 3) crossing the Kong Karl Platform, Bjarmeland Platform, Haapet Dome, Nordkapp Basin and Finnmark Platform.

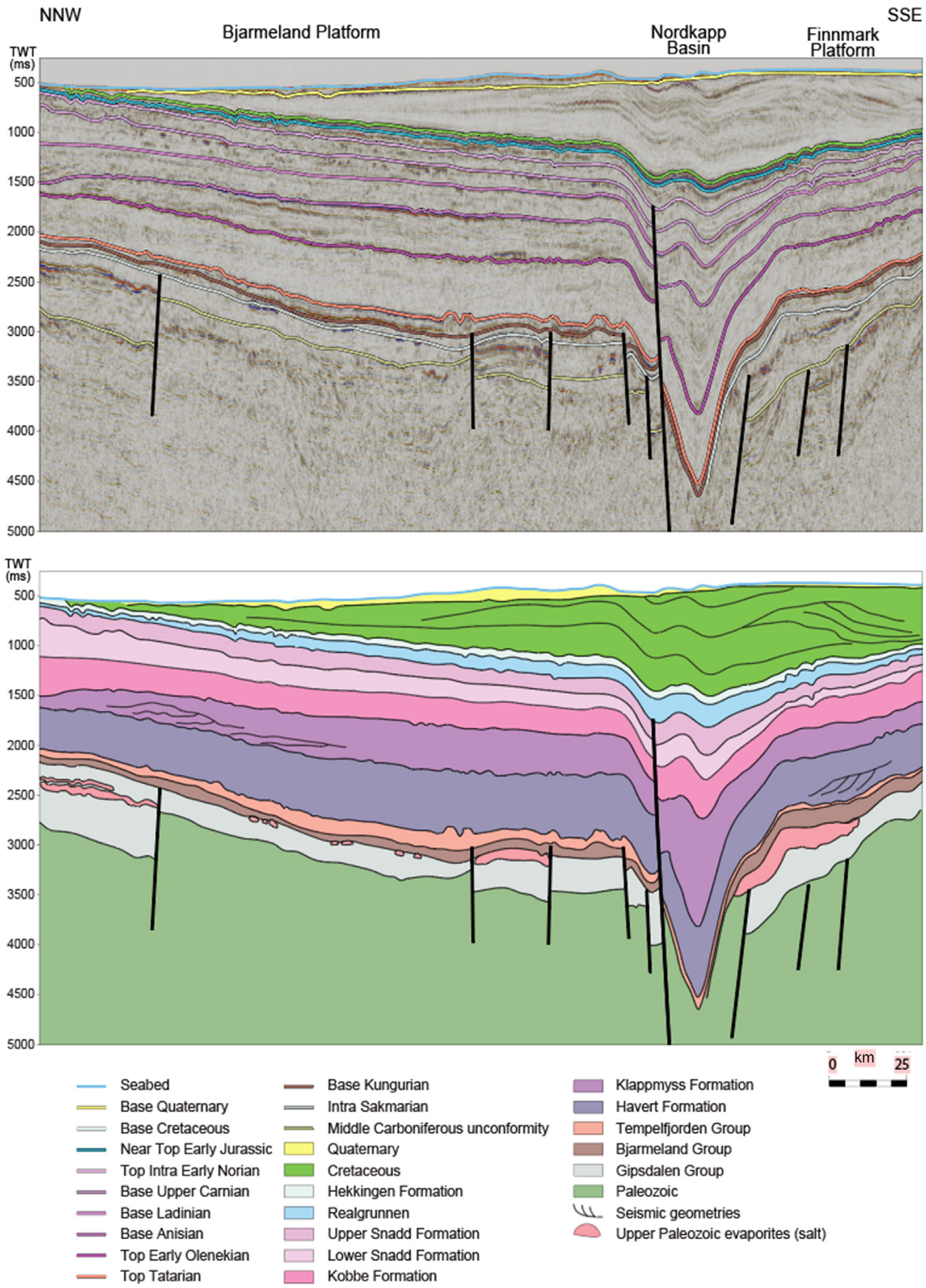

Fig. 10. North–south interpreted seismic line and geoseismic profile (line D in Fig. 3) over the Bjarmeland Platform, Norkapp Basin and Finnmark Platform. The seismic line is shown courtesy of TGS.

sides (Fig. 11). Its southwestern flank is bordered by an elongate salt-induced swell, the Signalhorn Dome (Figs 3 and 11), which has been tested by recent drilling (see the 'Current exploration status' subsection later in this paper). The Fedynsky High, a huge and subcircular basement palaeohigh, is essentially the remnant upstanding area between the Nordkapp Basin, the Tiddlybanken Basin and the monoclinal flank of the South Barents Basin. It is at least Late Paleozoic in age, as evidenced by unconformities in the Upper Paleozoic succession, and perhaps older. Doming and sediment pinchout onto the feature (e.g. of Lower Cretaceous strata) show that the high was frequently reactivated through time.

The platform area to the north of the Nordkapp Basin, the Bjarmeland Platform, is generally characterized by flat-lying strata dominated by several kilometres of Triassic sediments. At the western extremity of the area described, the Ottar Basin is a diffuse feature marking the continuation of the Nordkapp Basin into the Bjarmeland Platform and is separated from the basin by a basement high, the Norsel High. The Ottar Basin and environs are presumed to be characterized by thicker salt than elsewhere on the platform, supported by the presence of broad and significant salt swells (the Samson, Ververis, Norvarg and Svalis domes) and a salt-withdrawal syncline (the Maud Basin) in the west of the study area. The Svalis Dome (e.g. Gabrielsen *et al.* 1990) is of particular interest because it is truncated by Quaternary erosion such that Triassic and Permian strata exist at shallow depth in a circular subcrop pattern (Fig. 12), allowing these strata to be sampled and studied (e.g. Hochuli and Feist-Burkhardt 2004). Its peripheral sink (the Maud Basin: Fig. 13) creates an area where Triassic and Upper Jurassic source rocks are more deeply buried, and, hence, more capable of generating hydrocarbons.

In the NW of the Bjarmeland Platform, high-quality 3D seismic data show that shallow Jurassic and Triassic strata are criss-crossed by a complex array of normal faults (Fig. 13), which help to set up traps in the Wisting and

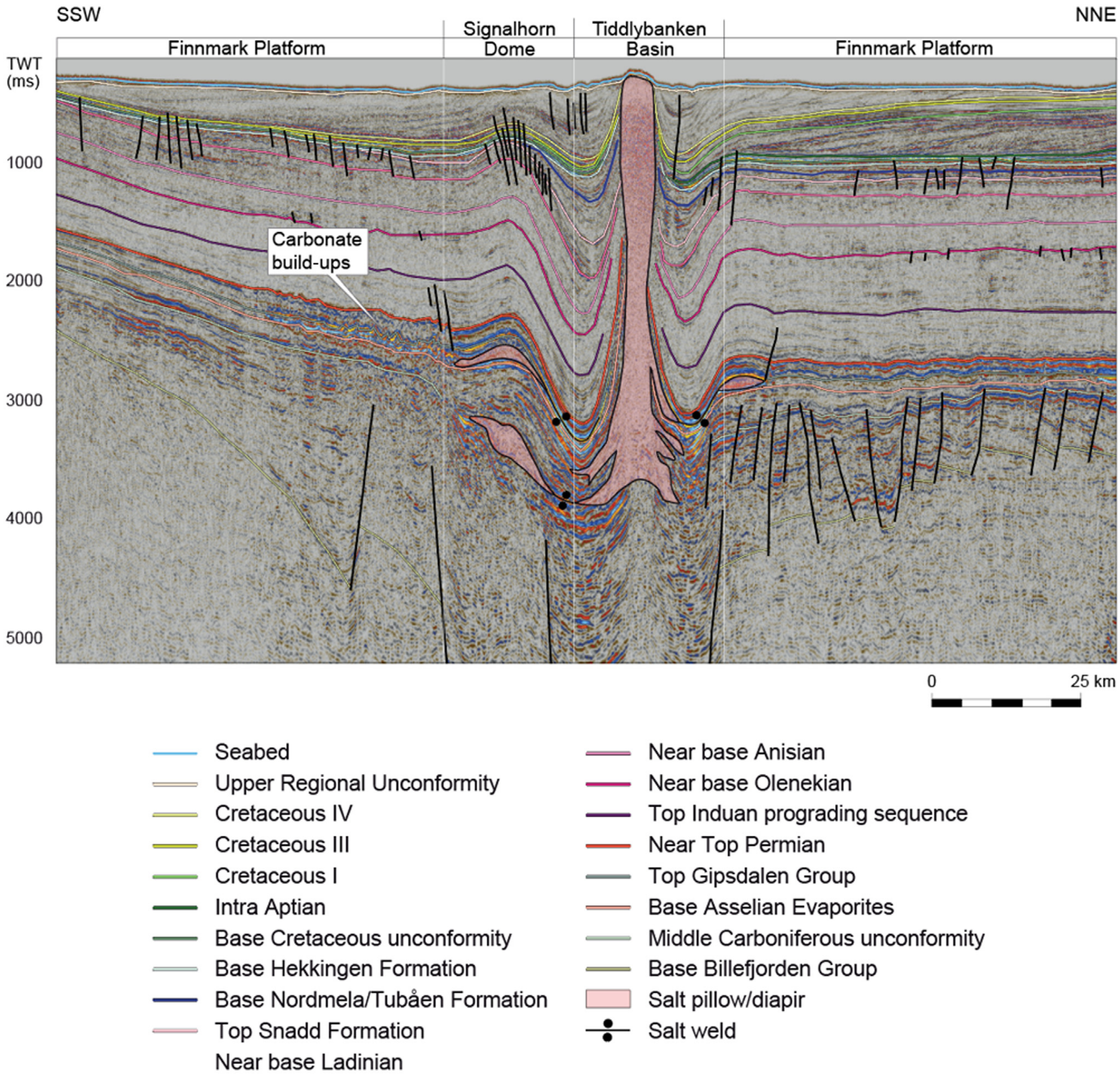

Fig. 11. NE–SW seismic line over the Tiddlybanken Basin (line E in Fig. 3) showing late Paleozoic basinal structure, salt withdrawal and multi-phase halokinesis. The recently drilled Signalhorn Dome and carbonate organic build-ups in the Permian interval are also clearly shown. The seismic line is shown courtesy of the Norwegian Petroleum Directorate (NPD).

Hoop areas. The faulting in this area appears to be multiphase, with small-scale Jurassic faults trending east–west or ENE–-WSW, similar to the trends in the Hammerfest Basin to the south. These faults are often truncated and/or offset by younger (probably Aptian) and larger normal faults trending NE–SW and north–south. The latter almost certainly reflect Early Cretaceous downfaulting and subsidence of the Barents Sea western margin, best seen in the Bjørnøya Basin and along the Bjørnøyrenna Fault Complex that bounds the Loppa High to the west.

In the northeasterly part of the platform, the Haapet Dome close to the Norway–Russia border (Fig. 3) occurs where a NW–SE-trending ridge (as defined at base Cretaceous level) intersects the northeasterly projection of the Nordkapp Basin. Although there is slight salt thickening beneath the dome, the main mechanism of formation is considered to be inversion. Detailed mapping of drape and thickness variations suggest that this process occurred in several episodes between the Triassic and Early Cretaceous.

The Bjarmeland Platform merges eastwards in the Russian sector into a major monocline (the Central Barents Monocline), plunging eastwards into the deep South Barents Basin (Drachev *et al.* 2021). The latter basin is part of the north–south-trending Barents Sea megabasin adjacent to the Novaya Zemlya islands, characterized by massive Permo-Triassic sedimentary infill (Henriksen *et al.* 2011*b*) (see also Figs 8 and 9). The precise cause of the immense sag basins west of Novaya Zemlya is unknown. They have been described as a foreland basin, a relict back-arc and/or as subsidence resulting from dense material in the upper mantle (e.g. Johansen *et al.* 1993; Ebbing *et al.* 2007; Ritzmann and Faleide 2009).

Mjølnir impact crater

Mjølnir is a well-resolved impact crater lying in about 200 m of water in the central part of the Bjarmeland Platform

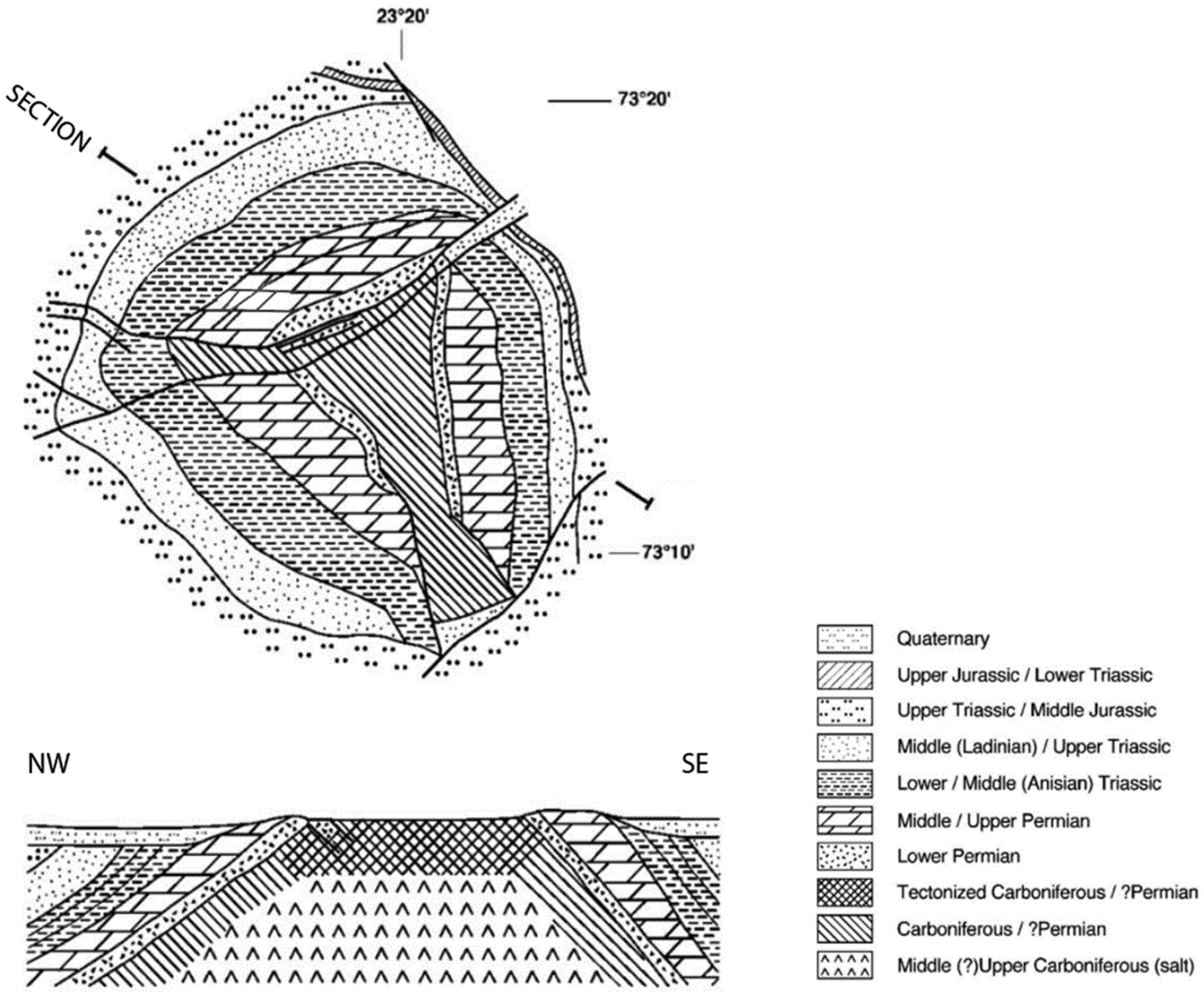

Fig. 12. Subcrop map and cross-section over the salt-induced Svalis Dome in the west of the TSE (line F in Fig. 3). Late movement on the structure has brought Triassic and late Paleozoic successions to shallow depth, and, hence, has provided a critical sampling point in the south-central Barents Sea. Figure adapted from Hochuli and Feist-Burkhardt (2004).

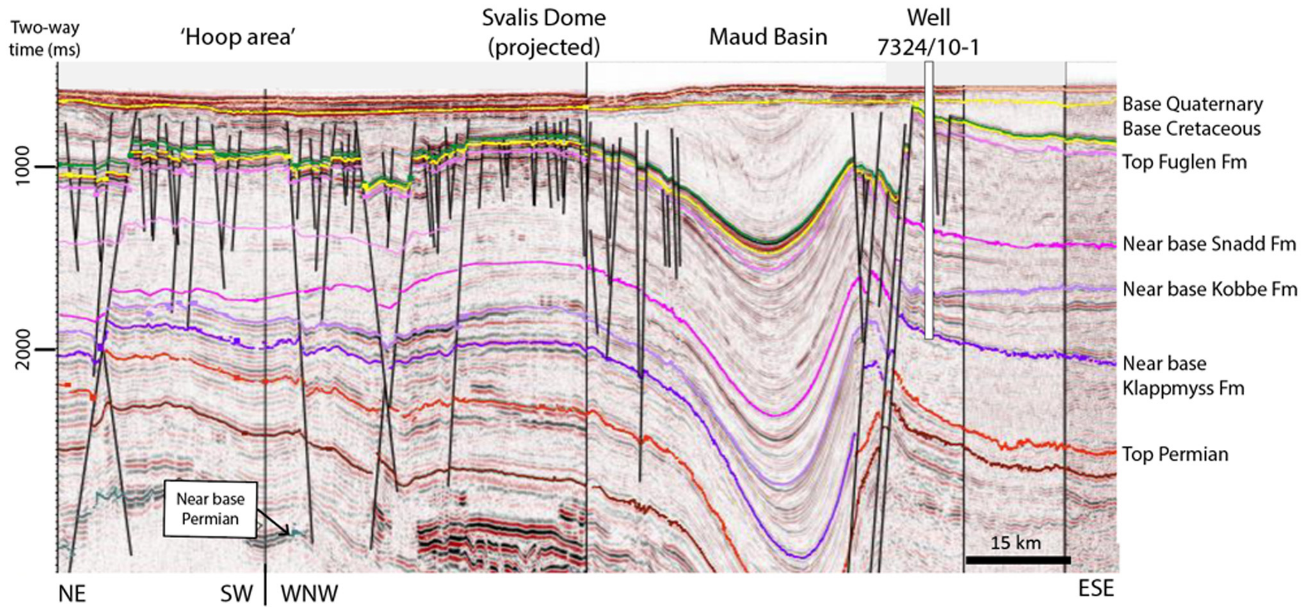

Fig. 13. Interpreted seismic line over the Maud Basin and Hoop area (line G in Fig. 3). The Maud Basin is a salt-withdrawal syncline associated with formation of the Svalis Dome. High reflectivity at depth in the projection of the Svalis Dome probably represents Carboniferous–Permian evaporites. Intense, generally small-scale extensional faulting of Late Jurassic–early Cretaceous age is well displayed on the left of the section. These faults are critical to trapping in the Wisting and Intrepid Eagle discovery area. The seismic line is shown courtesy of TGS.

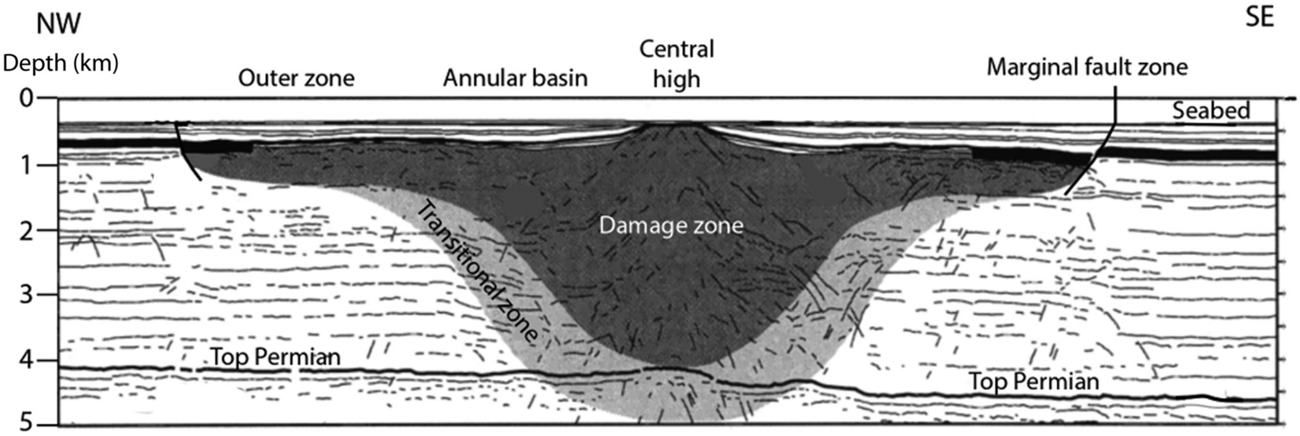

Fig. 14. Geoseismic profile over the Mjølnir impact structure (line H in Fig. 3). Figure adapted from Tsikalas (1996).

(Fig. 14). Since its original identification by Gudlaugsson (1993), an extensive dataset has been obtained over the feature, including high-resolution seismic, gravity and magnetic profiles, and detailed reports have been published (e.g. Tsikalas 1996). In the latter work, the crater was described as 40 km wide, although Werner and Torsvik (2010) considered it to have a smaller diameter of about 20 km. The impact appears to have taken place in a shallow-marine setting in Berriasian times (*c.* 142 Ma). Because of the marine setting, the crater is comparatively shallow, but otherwise has typical characteristics of an astrobleme, including a central raised portion, a damage zone to a depth of about 4 km and an ejecta apron (Fig. 14). Shallow drilling of nearby contemporaneous stratigraphy by IKU shallow borehole 7430/10-U-1 revealed shock quartz and high iridium values associated with the impact.

Sedimentary fill

Total thickness

The Base Permian map (Fig. 15), which is the earliest horizon that can be mapped regionally with some confidence, provides a good indication of the sediment thickness distribution in and around the south-central Barents Sea. The sedimentary fill is approximately 6–8 km, with the thickest developments in the axes of the rifts (Nordkapp and Tiddlybanken basins) (e.g. Figs 7–9). Farther east, the sediment thickness increases to 20 km or more in the South Barents Basin (Figs 7 and 8) (see also Drachev *et al.* 2021). To the south, sediments are truncated and thin to zero on the Finnmark Platform.

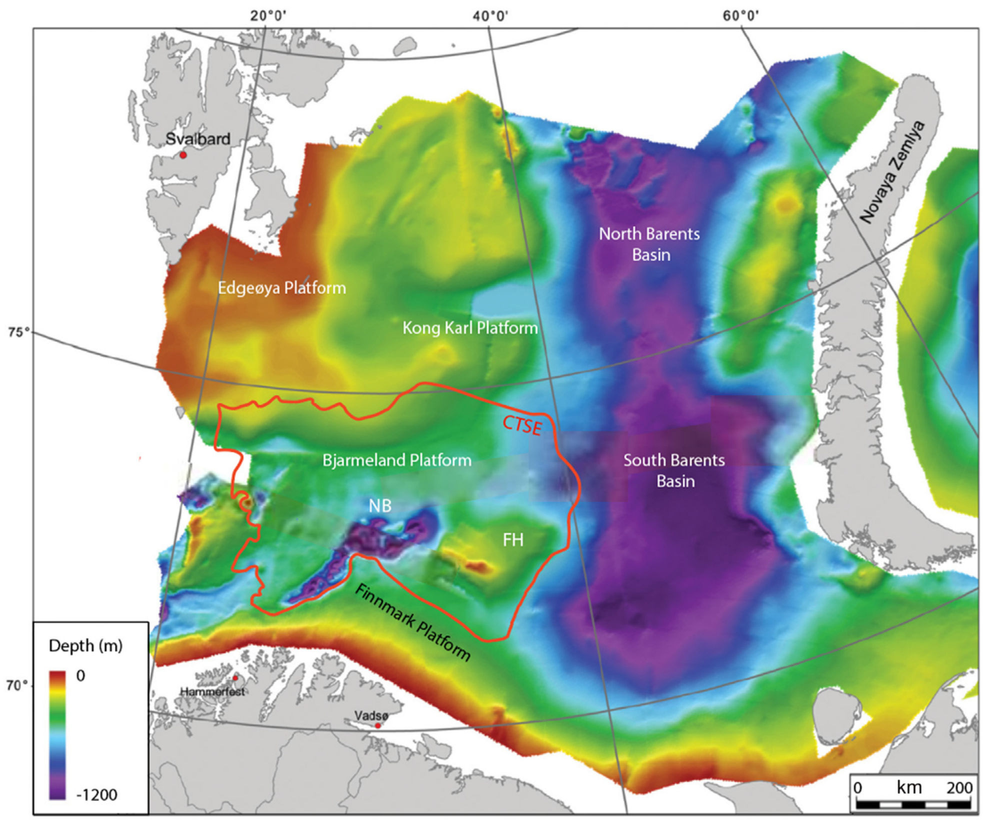

Fig. 15. Near Base Permian depth map of the Barents Sea, illustrating the sediment thickness distribution in and adjacent to the South-Central Barents Sea CTSE. Abbreviations: FH, Fedynsky High; NB, Nordkapp Basin. Modified after Henriksen *et al.* (2011*b*).

Lithostratigraphy/seismic stratigraphy

A standard lithostratigraphic nomenclature for the Mesozoic and Cenozoic successions of the Barents Sea was published by Dalland *et al.* (1988). Subsequently, Upper Paleozoic lithostratigraphy was covered by Larssen *et al.* (2002). A lithostratigraphic chart for the Barents Sea may be found on the Norwegian Petroleum Directorate website at https://www.npd.no/facts/geology/lithostratigraphy (NPD 2019*a*).

A more specific lithostratigraphy and chronostratigraphy for the South-Central Barents Sea CTSE is shown in Figure 4, along with related tectonic events and evolution of the petroleum system. Three megasequences, of Late Devonian–Late Permian, Early Triassic–Middle Jurassic and Late Jurassic–late Cretaceous ages, make up the bulk of the sedimentary fill. These units, their geometries, and their component groups and formations can be mapped over most of the study area, and are illustrated in the geoseismic sections of Figure 7–9. Confidence in the seismic mapping decreases somewhat in the Upper Paleozoic, because most well ties to this section are on the periphery of the area (Loppa High and Finnmark Platform). An exception is the 7226/11-1 (Norsel High) well, where Carboniferous Gipsdalen Group sediments overlie metamorphic basement. Depositional environments of the entire section are readily established from well penetrations, seismic stratigraphy, shallow cores and equivalent onshore outcrops (i.e. on Svalbard). They are described below.

Depositional environment and provenance

The lowermost megasequence, of late Devonian–Late Permian age, represents material accumulated in extensional, fault-bounded graben and subsequent thermal subsidence in those basins. Within this overall setting, the Billefjorden Group (Late Devonian–Early Carboniferous) comprises predominantly terrestrial sediments with coal-bearing strata, drilled locally on the Finnmark Platform (Bugge *et al.* 2002) and local red beds. These units are separated by a major unconformity from the overlying Gipsdalen Group (Late Carboniferous–Early Permian), which records a regional transition to a warm and arid/semi-arid climate. Sediments included red beds and carbonate platforms passing laterally into saline/evaporitic basins, with the thickest evaporite developments in the rift axes (Smelror *et al.* 2009). The succeeding Bjarmeland Group comprises cool-water carbonates, with organic build-ups dominated by bryozoans and later by siliceous sponges (Larssen *et al.* 2002). Siliciclastic input into the cool-water carbonate regime increased in the Late Permian Tempelfjorden Group due to evolving deformation in the Urals. This episode culminated with deposition of a widespread black shale, the Ørret Formation, identified as a potential source rock in eastern parts of the Barents Sea (Henriksen *et al.* 2011*b*).

The succeeding megasequence, of Early Triassic–Middle Jurassic age, overlies a significant unconformity (Fig. 4) and is the result of hinterland uplift and very high sediment flux that occurred over the entire Barents Sea, particularly in the east. The Sassendalen Group (Induan–Early Ladinian) comprises marine shales and terrestrial strata sourced primarily from the Uralian fold belt to the SE, and to a lesser degree from the Baltic Shield (e.g. Glørstad-Clark *et al.* 2011; Henriksen *et al.* 2011*b*; Klausen *et al.* 2015; Fleming *et al.* 2016; Eide *et al.* 2017; Flowerdew *et al.* 2019). Seismic mapping of shelf-edge clinoforms shows several phases of shelf/delta progradation from the east, within the Havert, Klappmyss and Kobbe formations (Fig. 16), separated from each other by marine flooding surfaces. Marine, black shales within the deltaic succession have significant source potential, and are described in the 'Source rocks' subsection later in this paper. The Sassendalen Group is the dominant unit of the study area, attaining thicknesses of the order of 2500 m on the Bjarmeland Platform and thickening westwards into the South Barents Basin. The basal Havert Formation, representing the initial influx of sediment from the Uralian deformation, records very fast deposition of 1–3 km of sediment in 1–2 myr.

The overlying Kapp Toscana Group (Ladinian–Bathonian) includes the main reservoir systems of the Barents Sea. It represents a persistence of fluvial, deltaic and marginal-marine conditions, but with gradual diminution of clastic supply due to waning Uralian influence and declining subsidence rate. The group is further divided into the Storfjorden and Realgrunnen subgroups, which reflect very different depositional settings (Dallmann 1999). The Storfjorden Subgroup (Ladinian–Early Norian Snadd Formation) records a widespread Ladinian transgression followed by significant delta progradation towards the NW (Lundschien *et al.* 2014; Klausen *et al.* 2019). It is characterized by widespread mudrocks including organic-rich shales, overlain by coal-bearing strata, but also contains channelized sandbodies sourced from the Uralian Orogen (Fleming *et al.* 2016; Flowerdew *et al.* 2019) capable of forming good reservoirs. A very limited supply of sediment from the south (Fennoscandia) has also been recorded on the Finnmark Platform.

The succeeding Realgrunnen Subgroup (Early Norian–Bathonian) comprises a Late Triassic unit (Fruholmen Formation) with a basal marine mudrock of Early Norian age, representing a significant marine transgression, followed by end-Triassic delta progradation (Ryseth 2014). The main sediment supply was from the SE, including the exhuming Novaya Zemlya fold belt (Klausen *et al.* 2016). An increased supply of clastic material from Fennoscandia is, however, recorded in the SE part of the CTSE, reflected by coarser and more quartz-rich sandstones deposited in the transition zone between the Hammerfest and Nordkapp basins (Bergan and Knarud 1993; Ryseth 2014). On a regional scale, uplift to the NW also created a new hinterland in northern Svalbard (Olaussen *et al.* 2018).

Early Jurassic strata rest unconformably on the Fruholmen Formation, and are generally coarser grained and typically enriched in quartz compared to the underlying Triassic strata, particularly in the western part of the CTSE. They reflect fluvial (Tubåen Formation) and tide-influenced (Nordmela Formation) deposition across the shelf, including the South Barents Basin. Sedimentary provenance data indicate that the southern part of the CTSE received sediment from northern Baltica (Flowerdew *et al.* 2019), whereas the northern part of the CTSE had a continued sediment input from the SE and Novaya Zemlya (Klausen *et al.* 2016). The uppermost Stø Formation, a significant reservoir unit in the western Norwegian Barents Sea, reflects Toarcian transgression and widespread shallow-marine deposition. It is commonly separated from the underlying units by a basal Toarcian unconformity and is, in turn, unconformably overlain by marine mudrocks of the Adventdalen Group.

The Early–Middle Jurassic sandstones appear to represent uplift of surrounding hinterlands, evidenced by significant unconformities below the Tubåen and Stø formations (Fig. 4), and data showing increased provenance from Fennoscandia (Klausen *et al.* 2017*a*, *b*). Furthermore, contemporary compressive tectonism in Novaya Zemlya (Olaussen *et al.* 2018; Müller *et al.* 2019) may have led to local uplifts in the flanking platform areas, with possible subaerial exposure enhancing the observed unconformities.

The uppermost megasequence (Middle Jurassic–Late Cretaceous), the bulk of which comprises the Bathonian–Cenomanian Adventdalen Group (Fig. 4), marks intensifying

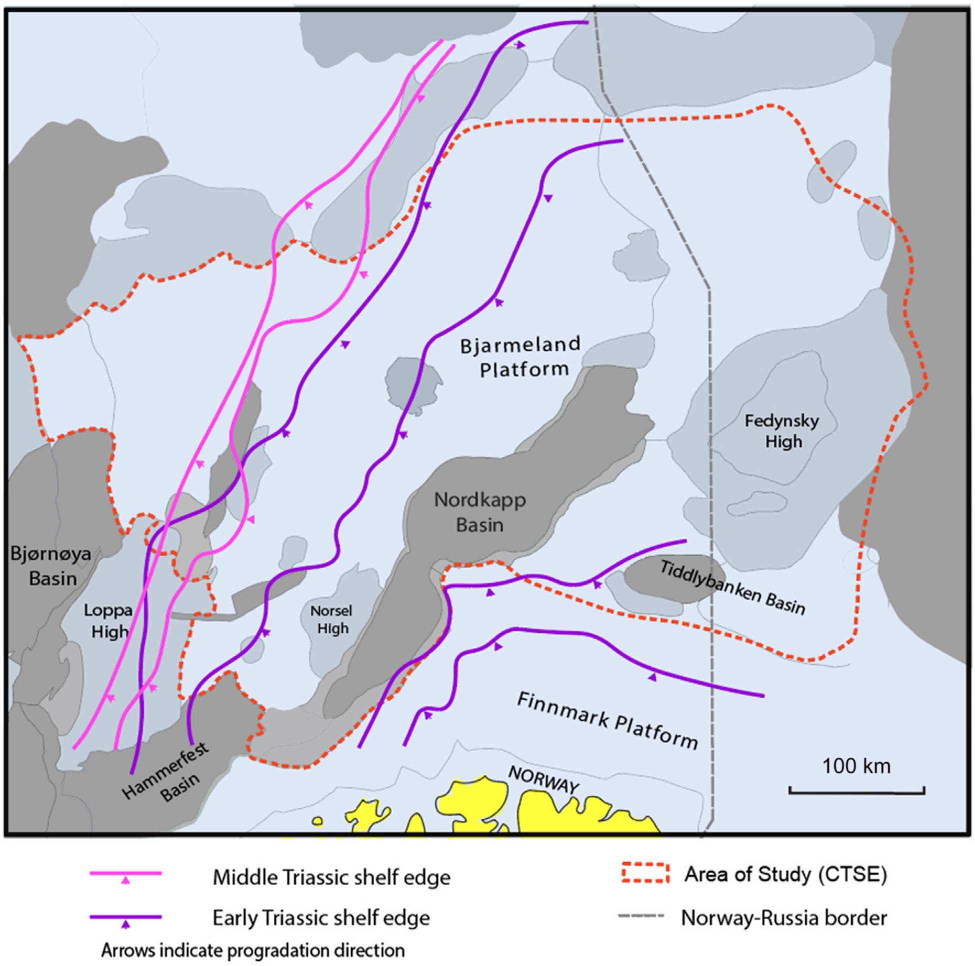

Fig. 16. Triassic shelf edges marked by downlapping clinoforms mapped on seismic. The shelf edges generally migrated across the TSE in a northwesterly direction. Shelf edges marked in purple are of Induan–Olenakian age, while those marked in pink are of Anisian–Ladinian age. Structural elements from Figure 3 are shown in greyscale for reference.

marine conditions with a major and widespread transgression across the entire Barents Sea. Regional marine anoxia in the Late Jurassic is reflected by the organically rich Hekkingen Formation in the Barents Sea, and in the correlative units in the South Barents Basin, Kara Sea and western Siberia (Bashenov Formation). The transgressive nature of the megasequence is also indicated by the presence of Bathonian–Kimmeridgian sediments unconformably overlying the folded strata onshore in the Novaya Zemlya archipelago to the east (Suslova 2013). The succeeding Lower Cretaceous sediments are dominated by marine mudrocks, but clinoforms observed on the Bjarmeland Platform indicate progradation from the north and the likelihood of coarser clastic facies (Midtkandal et al. 2020). To the east, Cretaceous rejuvenation of Novaya Zemlya and other eastern and northeastern provenance areas resulted in input of nearshore, sandy facies into the South Barents Basin (e.g. Stoupakova et al. 2011; Drachev et al. 2021).

Cenozoic sediments are thin to absent over the area. Where present, they comprise marine mudstones, occasional coarser clastics and (in the uppermost part) glaciomarine sediments. They reach a maximum of about 500 m in peripheral halokinetic sinks in the Nordkapp Basin.

Magmatism

The Late Paleozoic–recent history of the CTSE was surprisingly quiet in magmatic terms, given its proximity to large igneous provinces of Late Devonian (Kola Alkaline Province), Permo-Triassic (Siberian traps), Early Cretaceous (High Arctic Large Igneous Province (HALIP)) and Paleogene (North Atlantic Igneous Province (NAIP)) age.

In the far east of the study area, and eastwards into the Barents megabasin, numerous irregular sills are observed on seismic, mainly intruding the Triassic succession (Fig. 8) (also Drachev et al. 2021). This 700 000 km^2 sill complex extends northwestwards to Kong Karl's Platform and Svalbard, and appears to be a significant component of the larger HALIP, which stretches to NE Greenland and the Canadian Arctic islands (Enclosure D of this volume). Recent radiometric dating (e.g. Corfu et al. 2013; Polteau et al. 2016) suggests a narrow age range for the HALIP, with peak activity at about 125 Ma (earliest Aptian).

Heat flow

Heat flows were measured in the Nordkapp Basin area during the IKU shallow coring programme and published in Bugge et al. (2002). An exceptionally high heat flow of 104 mW m^{-2} was measured over one of the axial diapirs, reflecting the high conductivity of the underlying salt. Away from the basin axis and the halokinetic structures, values in the range 45–55 mW m^{-2} were obtained. These are fairly typical cratonic values (e.g. Goutorbe et al. 2011), probably reflecting the proximity of the Baltic Shield, and the comparatively unthinned nature of the crust and lithosphere in this part of the Barents Sea. Comprehensive modelling of present-day heat flow based on onshore measurements and offshore geophysical data has been performed by the NGU in the HeatBar project (Pascal et al. 2010). This project mainly concentrated on the SW Barents Sea; however, it appears to suggest values averaging 60 mW m^{-2} at the western edge of the CTSE, with peaks on the palaeohighs and troughs in the sedimentary basins.

A key issue in the CTSE, and for most of the Barents Sea, is the use of heat flow measurements in basin modelling. As indicated earlier, the south-central area underwent net erosion of up to 1500 m (e.g. Henriksen *et al.* 2011*a*; Ktenas *et al.* 2017). This means that currently recorded heat flows are likely to represent a disequilibrium condition due to geologically recent removal of sedimentary cover, and thus it is difficult to estimate palaeoheat flow. However, recent work by Klitzke *et al.* (2016) and Hokstad *et al.* (2017) represents a significant advance in the estimation of both regional and palaeoheat flow. In this methodology, mantle, crustal and sediment radiogenic heat-flow values are estimated from geophysical (gravity and magnetic) and rock physics data, and the Barents Sea is used as a case study. In theory, this indirect method of inverting heat flow holds the potential to estimate maturity, generation and migration through time, an understanding of which has previously been lacking in the Barents Sea.

Petroleum geology

Discovered and potential petroleum resources

The area is sparsely explored and, although some 17 petroleum discoveries are documented, only one (Wisting) is likely to undergo development in the next few years. Discoveries and key exploration wells are shown in Figure 2. All exploration wells drilled in the CTSE, and their results, are shown in Table 1.

Wisting (well 7324/8-1) and its satellite Hanssen (well 7324/7-2), in the Hoop Fault Complex on the Bjarmeland

Table 1. *Petroleum discoveries to date in the South-Central Barents Sea CTSE*

Year (spud)	Well	Structural element	Target reservoir (age)	Results	Main unit with hydrocarbons	Name (discovery)
1987	7124/3-1	Nysleppen Fault Complex	Carboniferous–Middle Jurassic	Oil/gas discovery	Realgrunnen Subgroup	Bamse
1987	7226/11-1	Norsel High	Permian–Early Jurassic	Gas discovery	Havert Formation	Norsel
1988	7224/7-1	Samson Dome	Permian–Middle Jurassic	Dry with gas shows	Kobbe Formation	
1988	7125/1-1	Nysleppen Fault Complex	Middle Triassic–Jurassic	Oil/gas discovery	Kobbe Formation, Realgrunnen Subgroup	Binne
1989	7324/10-1	Maud Basin	Early–Middle Triassic	Dry with shows	Snadd Formation	
1989	7228/2-1S	Nordkapp Basin	Middle Triassic–Middle Jurassic	Dry with oil shows	Realgrunnen Subgroup	
2001	7228/7-1	Nordkapp Basin	Late Triassic	Oil/gas discovery	Klappmyss and Snadd formations	Pandora
2006	7227/11-1	Nordkapp Basin	Late Triassic	Dry with gas shows	Gipsdalen Group	
2007	7125/4-1	Måsøy Fault Complex	Middle Triassic–Middle Jurassic	Oil/gas discovery	Kobbe Formation, Realgrunnen Subgroup	Nucula
2008	7226/2-1	Bjarmeland Platform	Middle Triassic–Middle Jurassic	Gas Discovery	Kobbe Formation	Ververis
2008	7224/6-1	Bjarmeland Platform	Middle Triassic–Middle Jurassic	Gas discovery	Kobbe Formation	Arenaria
2008	7223/5-1	Bjarmeland Platform	Middle–Late Triassic	Gas discovery	Kobbe and Snadd formations	Obesum
2011	7225/3-1	Norvarg Dome	Permian–Middle Jurassic	Gas Discovery	Havert, Kobbe and Stø formations	Norvarg
2012	7228/1-1	Bjarmeland Platform	Late Triassic–Early Jurassic	Dry		
2013	7324/8-1	Hoop Fault Complex	Early–Middle Jurassic	Oil discovery	Realgrunnen Subgroup	Wisting
2013	7324/7-1S	Hoop Fault Complex	Middle–Late Triassic	Dry with shows	Kobbe and Snadd formations	
2014	7324/2-1	Hoop Fault Complex	Late Triassic–Middle Jurassic	Dry		
2014	7324/7-2	Hoop Fault Complex	Late Triassic–Middle Jurassic	Oil discovery	Realgrunnen Subgroup	Hanssen
2014	7324/9-1	Mercurius High	Late Triassic–Middle Jurassic	Gas discovery	Realgrunnen Subgroup	Mercury
2014	7325/1-1	Hoop Fault Complex	Early–Late Triassic	Gas discovery	Snadd Formation	Atlantis
2014	7227/10-1	Nordkapp Basin	Middle–Late Triassic	Dry		
2014	7125/4-3	Måsøy FC	Early Cretaceous	Dry		
2015	7124/8-2	Hoop Fault Complex	Late Triassic–Middle Jurassic	Dry with shows	Realgrunnen Subgroup	
2017	7435/12-1	Haapet Dome	Late Triassic - Middle Jurassic	Gas discovery	Realgrunnen Subgroup	Korpfjell
2017	7325/4-1	Hoop Fault Complex	Late Triassic–Middle Jurassic	Oil/gas discovery	Snadd Formation, Realgrunnen Subgroup	Gemini
2018	7324/3-1	Bjarmeland Platform	Not available	Gas discovery	Snadd Formation, Realgrunnen Subgroup	Intrepid Eagle
2019	7132/2-1	Tiddlybanken Basin	Not available	Dry		
2019	7324/6-1	Bjarmeland Platform	Not available	Oil discovery	Triassic	Sputnik

Platform, are promising light oil discoveries at shallow depth. They have Upper Triassic–Middle Jurassic reservoirs, probably sourced by adjacent and locally mature Triassic or (possibly) Upper Jurassic shales in the Maud Basin. With recoverable resources currently estimated to be in excess of 400 MMbbl, it is by far the most likely commercial development in the area and would thus constitute Norway's most northerly oil development. Five appraisal wells have been drilled and development solutions are currently being considered. A further small oil discovery, Sputnik (well 7324/6-1), was recently announced. It lies about 30 km NE of Wisting and has a Triassic reservoir. Other discoveries to date on the Bjarmeland Platform are mainly gas with occasional oil shows, probably sourced from the Triassic. They include the Mercury (well 7324/9-1), Norvarg (well 7225/3-1), Ververis (well 7226/2-1) and Arenaria (well 7224/6-1) accumulations on the western part of the platform. These discoveries are mainly in Triassic reservoir rocks, although minor Jurassic gas occurs in Mercury and Norvarg. In the far NW, a complex of shallow gas discoveries, including Intrepid Eagle and Atlantis, have mainly Jurassic (Realgrunnen Subgroup) reservoirs. The recently drilled Korpfjell discovery (well 7435/12-1) in the far NE of the area is a minor gas accumulation, mainly in the Lower Jurassic Nordmela Formation of the Realgrunnen Subgroup.

Minor gas and oil accumulations (e.g. the Nucula, Bamse and Binne fields) have been discovered in the southwestern Nordkapp Basin, at its junction with the Hammerfest Basin (Fig. 2). Nucula (wells 7125/4-1 and 7125/4-2) has reservoirs in both the Upper Triassic–Jurassic (Realgrunnen Subgroup) and Lower–Middle Triassic (Kobbe Formation) containing hydrocarbons probably migrated from Upper Jurassic source rocks to the west, and from local Triassic source rocks. Bamse (well 7124/3-1) and Binne (well 7125/1-1) have Realgrunnen Subgroup reservoirs and, again, were probably sourced from both the Upper Jurassic and the Triassic.

A modest-sized gas field (7226/11-1 structure) has been found on the in the Lower Triassic Havert Formation on the Norsel High, on the NW flank of the Nordkapp Basin. Farther NE in the Nordkapp Basin, the Pandora well (7228/7-1) found oil and gas in sands of the Middle–Upper Triassic Snadd Formation, and gas in the Lower Triassic Klappmyss Formation. Both accumulations are assumed to be sourced from the Triassic or possibly Upper Permian, and are trapped as abutments against salt diapirs.

Given the lightly explored nature of the south-central Barents Sea, and the existence of proven Jurassic and Triassic petroleum systems, more discoveries are likely in the area. Based on play analysis, NPD estimates that 1.165 BSm^3 (7.3 bbl) oil equivalent remain to be found in the southern Norwegian Barents Sea (i.e. south of 74° 30′ N), some 29% of Norway's remaining resource (http://www.npd.no/en/Publications/Resource-Reports/2018) (NPD 2018). However, this quite optimistic view should be tempered by two factors. Firstly, the southern Norwegian Barents Sea resource calculations also include prospective areas to the west of the CTSE, such as the Hammerfest Basin, Loppa High, Fingerdjupet Sub-basin and Bjørnøya Basin. Secondly, based on the evidence to date, gas is likely to predominate within the CTSE. The likely habitat of yet-to-find resources in the south-central Barents Sea is covered in the 'Hydrocarbon systems and plays' subsection later in this section.

Current exploration status

Despite the limited exploration success to date, the area is endowed with a wide range of potential reservoirs, source rocks and traps (see the following subsections). Optimism for future significant discoveries is reflected in the recently active licence and work programmes.

A treaty between Russia and Norway on maritime delimitation and collaboration in the Barents Sea and the Arctic Ocean came into force on 7 July 2011. Leasing of the Russian part of the formerly disputed zone to the Russian company Rosneft took place in 2012, and shortly afterwards international companies were brought into the area as joint venture partners. The leasing included the Russian part of the giant Fedynsky High and, in contrast to current Norwegian policy, extended north of the 74°30' N limit of Norwegian exploration. The work programme in the area has been slow due to the effect of sanctions between the USA and Russia over the Ukraine conflict, and no drilling has yet taken place.

Following the Russia–Norway treaty, preparatory work in the Norwegian part of the formerly disputed zone included extensive 2D seismic reprocessing and broadband 3D seismic acquisition (Fig. 2), together with local electromagnetic (EM) seabed surveys. Extensive leasing of the area, together with other parts of the eastern Norwegian Barents Sea, took place in the Norwegian 23rd Licensing Round in May 2016. At the time of writing, drilling has taken place in the Haapet Dome area, resulting in a small Jurassic gas discovery, Korpfell. A later, deeper Triassic test in this area (well 7335/3-1) did not discover significant hydrocarbons. Farther south, shallow (Jurassic) and deep (Triassic) tests on the Signalhorn Dome, flanking the Tiddlybanken Basin (the Gjøkåsen prospect, wells 7132/2-1 and 7132/2-2) both failed to find hydrocarbons.

Hydrocarbon systems and plays

Source rocks. Source-rock potential exists in the area over a wide stratigraphic range, including in the Permo-Carboniferous, at several levels of the Triassic and in the Upper Jurassic (Fig. 4). The Wisting oil discovery in the west of the area is probably sourced from locally mature Triassic or possibly Upper Jurassic source rocks in the adjacent Maud Basin. The Upper Jurassic also contributes to the Nucula, Bamse and Binne accumulations in the SW. Elsewhere in the area, where the Upper Jurassic is immature, the Triassic is expected to be the principal source.

Permo-Carboniferous. Early Carboniferous continental source-rock developments have been proven regionally, for example on the Finnmark Platform (e.g. Bugge *et al.* 2002; Van Koeverden *et al.* 2010; Henriksen *et al.* 2021*a*) and on Svalbard (Abdullah *et al.* 1988; Van Koeverden *et al.* 2011). The Carboniferous coal and coaly shales contain gas-prone Type III kerogen with some local mixed Type II/III. Oil-prone Visean coals are observed in wells on the Finnmark Platform.

High seismic amplitudes in basinal settings in the Upper Carboniferous–Lower Permian Gipsdalen Group suggest that this unit could have source potential in the eastern Norwegian Barents Sea. The Ørn Formation sediments of this group, on the Finnmark Platform, reflect deposition on a restricted shallow carbonate shelf. Siltstones interbedded with the carbonates show up to 5% total organic carbon (TOC) and hydrogen indices (HI) of 100–320 mgHC g^{-1} TOC, suggesting good potential for oil and gas generation.

Marine shales and siltstones of the Upper Permian Ørret Formation (Tempelfjorden Group) are proven in the western Barents Sea and on the Finnmark Platform. The unit is 80–120 m thick with 1–4% TOC, Type III to Type IV organic matter and, where penetrated, little remaining generation potential. Seismic amplitude work, however, shows that this unit may have additional source potential on parts of the

Bjarmeland Platform, and in the axes of the Nordkapp and Tiddlybanken basins.

Lower Triassic. Mudstones within the alluvial plain deposits of the Early Triassic (Induan–Olenekian) Havert and Klappmyss formations show good to excellent source-rock richness and mainly Type III gas-prone kerogen in parts of the eastern Barents Sea, but no significant potential in the Nordkapp Basin and on the Finnmark Platform. Seismic interpretation and amplitudes are consistent with good source-rock development in the Tiddlybanken Basin, where this source-rock interval may reach a thickness of 20–30 m.

Middle Triassic. Source rocks of Anisian and Ladinian age are proven in the Nordkapp Basin, on the Bjarmeland and Finnmark platforms, and in the South Barents Basin. Deposition occurred in a marginal-marine to deltaic/coastal plain setting. The shale and siltstone of the Kobbe Formation (Anisian age) is dominated by Type III kerogen and shows fair to good gas potential. TOC concentrations exceed 1% in large parts of the succession, with thicker, richer intervals containing Type II/III kerogen, representing marine flooding incursions. These source rocks have good potential to generate gas-condensate and/or light oil. They appear to become thicker and richer towards the Loppa High in the west. The Kobbe Formation is time-equivalent to the Botneheia Member of Svalbard, a unit of known high source potential for oil and gas (e.g. Bjorøy *et al.* 1978). The organic-rich character persists eastwards into the Russian sector, where TOCs of 1–7% are recorded in Fermanovskoe, Severo-Kindinskoe and Murmanskoe.

Upper Triassic. The upper Snadd Formation (Carnian) and its Russian time-equivalents include carbonaceous shales, coals, siltstones and sandstone deposited in coastal plain, deltaic and shallow-marine environments. Excluding the coals, TOCs of up to 9% are recorded in the Norwegian sector, and up to 15% in the Russian sector. Mixed Type II and III kerogens, with good to excellent gas-condensate potential and moderate oil potential are identified in the Nordkapp Basin, on the Finnmark and eastern Bjarmeland platforms, and in the South Barents Basin of the Russian sector (e.g. Klett and Pitman 2011).

Upper Jurassic. The regionally significant source rock, the Oxfordian–Tithonian Hekkingen Formation, is proven on the Bjarmeland Platform, Nordkapp Basin and the Finnmark Platform, but is absent on the southern Finnmark platform. Deposition occurred in a deep-marine to shelfal environment with dysoxic to anoxic bottom water conditions. Its thickness is 30–55 m where drilled. It is a rich source rock, with TOCs averaging 7% and HIs in the order of 270 mgHC g^{-1} TOC. It contains Type II and III kerogen, and has good to excellent oil and gas potential.

Upper Jurassic black shales (Kimmeridgian–Tithonian) are also present in the southern Russian Barents Sea. They are as rich as their Norwegian equivalents, with TOCs in the range of 8–16%, and contain sapropelic/humic kerogens.

Maturities. Upper Jurassic source rocks are expected to be too shallow to be mature over all of the area described, although the small accumulations in the west (e.g. Nucula) probably received Upper Jurassic hydrocarbons migrated from mature areas farther west. Triassic source rocks are probably at early–late oil-window depths over much of the area, with greater maturities in the axes of the Nordkapp and Tiddlybanken basins. Potential Permo-Carboniferous source rocks are at immature oil-window maturity levels where drilled, but are expected to attain dry gas or post-mature levels in the basin axes.

As indicated earlier, the area was uplifted and eroded at several intervals during the Cenozoic, culminating in considerable denudation during the Quaternary glaciations. Thus, the currently observed maturity levels of the source rocks will reflect a previous, greater burial depth and higher palaeotemperatures. Preservation of accumulated petroleum is therefore a risk over the entire area, with this risk probably diminishing eastwards. For a description of some effects of exhumation on petroleum systems, see Doré *et al.* (2002).

Reservoirs. Reservoir developments ranging from the Late Paleozoic to the Early Cretaceous are possible in the area (Fig. 4). However, the most likely units to form viable plays are of Triassic and Jurassic age. The NPD has systematically mapped the areal distribution of potential plays in the area, and these maps may be found at http://www.npd.no/en/topics/geology/geological-plays/ (NPD 2019*b*).

Permo-Carboniferous. These strata are widespread in the south-central Barents Sea, and can be correlated to outcrops on Svalbard (e.g. Dallmann 1999) and Franz Josef Land (Dibner 1998). Potential reservoirs are present in the Early Carboniferous terrestrial and marginal-marine sandstones of the Billefjorden Group, in carbonate build-ups within the Late Carboniferous–Early Permian Gipsdalen Group (mainly Ørn Formation), and in Late Permian biogenic, spiculitic cherts in the Røye Formation of the Tempelfjorden Group (e.g. Bruce and Toomey 1993) (Fig. 5). However, the Upper Paleozoic rocks have generally been buried too deeply to preserve significant reservoir quality. An exception is on the Finnmark Platform (Henriksen *et al.* 2021*b*), where the units shallow and eventually subcrop, and where well 7128/4-1 found a minor oil accumulation in Røye Formation spiculites. In the core of the Fedynsky High, the Top Permian is at approximately 3500 m and conceivably at viable exploration depths, although the earlier additional burial by up to 1500 m prior to late exhumation adds significant risk.

Lower Triassic–lowermost Upper Triassic. Triassic units dominate the stratigraphy of the south-central Barents Sea and contain numerous potential reservoir levels within the depth range for drilling. These include submarine fans overlying deltaic and marginal-marine deposits in the Early Triassic (Induan–Early Olenekian) Havert Formation, terrestrial–marginal-marine sandstones of the Olenekian–Early Ladinian Klappmyss and Kobbe formations, and channelized and shallow-marine sands of the Late Triassic (Carnian–Early Norian) Snadd Formation. All the Triassic sediments, particularly the Havert Formation, reflect rapid basin subsidence and large sediment influx from hinterlands to the east and south. The depth range for the Triassic reservoirs (*c.* 1500–5000 m) reflects both the variability and great thickness of the Triassic deposits. Maximum burial depths and thicknesses are recorded east of the study area, where the base of the Triassic plunges to 12 km or more (Drachev *et al.* 2021).

As indicated above, hydrocarbon-bearing Triassic reservoirs occur in the Nucula, Norsel and Pandora fields within the study area. The Triassic also hosts several gas accumulations on the Bjarmeland Platform: for example, in the Norvarg, Ververis and Arenaria fields.

In the Lower Triassic, reservoir-quality sands are normally confined to the upper part of the Havert Formation. Porosity and permeability (poroperm) are generally low (2–15% and 0.1–1 mD, respectively) due to the fine-grained nature of the sediments and the high clay content. Large burial depths and maximum palaeotemperatures of over 120°C also reduce reservoir quality. The Klappmyss Formation is mainly prospective where developed as marginal-marine sandstones, with porosities of 16–25% and permeabilities in the 10–100 mD range. Quartz cement is the main poroperm-reducing agent, particularly where the unit's maximum burial prior to exhumation was large: for example, in the Nordkapp Basin. Calcite cementation also reduces poroperms. The more terrestrial Kobbe Formation, characterized by mouth-bar and delta-plain channels, has a higher detrital clay content, which generally reduces reservoir quality. Porosities of 15% are rarely exceeded but are required to attain even modest permeability levels (>1 mD). The Middle–Upper Triassic Snadd Formation has the best reservoir quality, and is also situated at the most ideal exploration depths. Reservoir quality is highly variable, but is best in channelized sandbodies, attaining porosities of over 20% and permeabilities of >100 mD in the Nordkapp Basin and on the Finnmark and Bjarmeland platforms. Clay coatings (typically chlorite) commonly occur in the Snadd Formation, and can preserve good reservoir quality to a maximum burial of approximately 3500 m (*c.* 140°C).

Upper Triassic–Middle Jurassic. As indicated above, the terrestrial–shallow-marine Realgrunnen Subgroup (Fig. 4) is an important reservoir in the Barents Sea, and constitutes a proven reservoir in the west of the area (Wisting, Nucula, Bamse and Binne). Farther east it is not a regular exploration target, but was tested in the small Korpfjell gas discovery in the NE. The unit is locally at prospective depth (*c.* 800 m) in other parts of the newly leased areas of the Norwegian sector,: for example, in the rim synclines and flanks of the Tiddlybanken Basin.

The thickness of the subgroup is highly variable. It is approximately 100 m thick over the Bjarmeland and Finnmark platforms, thinning southwards towards the present-day Norwegian landmass. It thickens to as much as 500 m in the rim synclines of the Nordkapp and Tiddlybanken basins. Its constituent formations are the Fruholmen Formation, comprising prodelta mudrock and mouth-bar/delta-plain deposits, succeeded by sandstone-dominated fluvial strata (Tubåen and Nordmela formations), and subsequently by shallow-marine sandstones of the Stø Formation. The subgroup spans the Triassic–Jurassic boundary, with the Fruholmen Formation dated as Norian, and the later formations spanning the interval to the Bajocian. For a fuller description of these units, see Ryseth (2014). Equivalent sediments are also present to the east in the South Barents Basin (e.g. Stoupakova *et al.* 2011), where the unit ranges in thickness from 400 to 1000 m, and includes the important Callovian gas reservoirs of the Shtokmanovskaya and Ludlovskaya fields.

Because of shallow burial and only moderate exhumation in the area, porosities and permeabilities in the best sands of the Realgrunnen Subgroup are highly favourable, with Darcy-scale permeabilities and porosities in the 20–30% range.

Lower Cretaceous. Cretaceous rocks are generally shallowly buried in the area and are dominated by marine mudrocks. Hence, they are not regarded as viable reservoir targets. However, on the Bjarmeland Platform, Lower Cretaceous strata of the Adventdalen Group are notable for marked clinoforms indicating progradation from the north. This progradation reaches as far south as the Nordkapp Basin, with the potential for sandy facies. East of the study area, clinoforms indicate a further major progradation into the South Barents Basin from easterly and northeasterly sources, with minor input from the Baltic Shield (e.g. Stoupakova *et al.* 2011; Drachev *et al.* 2021).

Seals. The top seal to the Upper Triassic–Middle Jurassic Realgrunnen Subgroup consists of the widespread and transgressive marine shales of the Fuglen and Hekkingen formations (Middle–Upper Jurassic) (Fig. 4). The combined thickness of the two units ranges from tens of metres to around 300 m.

Mudrocks are the dominant facies of the entire Triassic succession, providing multiple opportunities for intraformational seals (Fig. 4). In the Nordkapp Basin, abutment against Carboniferous–Permian diapiric halites is the dominant sealing mechanism in the Pandora accumulation (7228/7-1). A similar configuration may be present in the smaller Tiddlybanken Basin.

Traps. The probable timing of trap formation in the CTSE is shown in Figure 4. Although the number of proven traps in the South-Central Barents Sea TSE is limited, potential exists for a wide range of trap types in newly allocated and open acreage. These trapping styles, proven and potential, are shown schematically in Figure 17, and are described below.

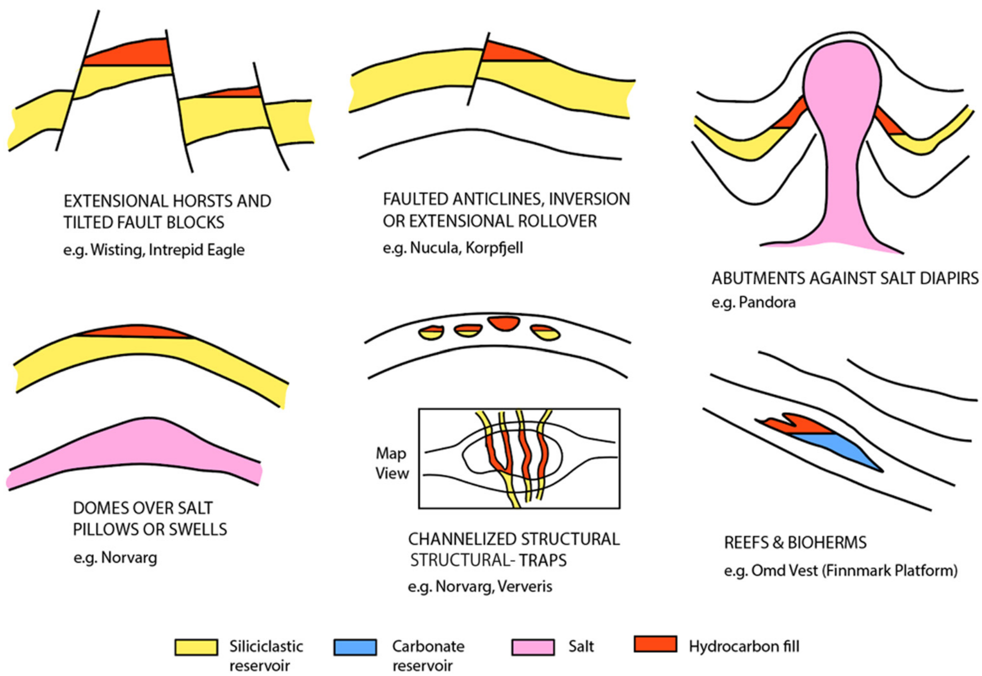

Fig. 17. Schematic sketches of the principal trapping styles, proven and postulated, with example discoveries in the South-Central Barents Sea Composite TSE.

Extensional rollover anticlines and fault traps. These are primarily associated with Mid-Jurassic–early Cretaceous extension. In the west and NW of the study area, shallow horsts and tilted fault blocks set up trapping in the Wisting oil discovery and in the small gas accumulations of the Hoop area (Atlantic, Intrepid Eagle). The faulting is complex but primarily characterized by ENE–WSW and east–west Jurassic faulting imprinted by younger (probably Aptian) and larger NE–SW and north–south normal faults. This extensional phase also created the traps of the Nucula, Bamse and Binne fields at the southwestern margin of the area. Such traps will be of lesser or no importance in the east of the area because of the diminishing eastward effects of the Jurassic extension.

Closure over salt swells, pillows and domes. These include simple traps at multiple Triassic and Jurassic levels. Fields such as Norvarg and Ververis to the NW of the study area occur above gentle, non-penetrative salt swells.

Abutments against diapiric salt. In the Nordkapp and Tiddlybanken basins, the salt penetrates to surface and, hence, truncates potential reservoirs of Triassic–Cretaceous age. Halite is an almost perfect seal and, hence, there is the potential for significant hydrocarbon columns. In the Pandora (7228/7-1) oil and gas discovery, inferred columns in the Triassic reservoirs are in the order of 500 m, but the steepness of the dipping reservoir limits areal size. Unlike many halokineic basins worldwide, seismic demarcation of the salt–sediment interface in the Nordkapp Basin abutments is difficult because of the similar interval velocities of the Triassic rocks (c3.5–4.5 m s^{-1}) and the halite (*c.* 4.5 m s^{-1}) (E. Henriksen pers. comm.).

Closures related to inversion, drape over palaeohighs or both. The largest of these, the Fedynsky High that straddles the Norwegian–Russian border, is at least as old as late Paleozoic and was reactivated in the early Cretaceous. The Haapet Dome, located where the Bjarmeland Platform traverses the border, is an inversion feature with some salt involvement (see the earlier 'Subdivision and internal structure' section in this paper). Detailed mapping of drape and thickness variations suggest episodic inversion between the Triassic and Early Cretaceous, creating trapping potential at Triassic and Jurassic levels. The recent Korpfjell gas discovery on this structure is probably controlled by drape, faulting and stratigraphic trapping. The Norsel High, containing the small 7226/11-1 gas discovery, is also essentially a palaeohigh, comprising part of the northwestern rift flank of the Norkapp Basin. In the Russian sector to the west, giant gas discoveries of the South Barents Sea Basin, such as Shtokmanovskaya, are domes representing gentle compression of the thick sedimentary pile. Inversion was initiated in the Jurassic, peaked in the early Cretaceous and was reactivated in the early Cenozoic.

Stratigraphic and structural-stratigraphic traps within the Triassic succession. The terrestrial and deltaic regime of the pre-Realgrunnen Subgroup Triassic means that Triassic sandbodies are often channelized. Thus, there is a stratigraphic element in most Triassic discoveries to date (particularly evident in the Ververis gas discovery on the Bjarmeland Platform) and similar geometries are likely to occur in new Triassic tests in the study area.

Carbonate build-ups within the Late Paleozoic succession. Early Carboniferous–Late Permian bioherms are documented in the area (Bruce and Toomey 1993) and have been tested as a trap on the Finnmark Platform. They could conceivably form traps on the flanks of the Nordkapp and Tiddlybanken basins but over most of the area are buried deeply and/or have been very deeply buried in the past, making them at best a secondary target.

Acknowledgements Many thanks to Harald Brekke, Sergey Drachev and Erik Henriksen, whose constructive reviews improved the paper and provided additional insights into this fascinating area of continental shelf. Thanks also to Albina Gilmullina for some important proof-stage corrections.

Author contributions **AGD**: writing – original draft (lead); **TD**, **MJF**, **TF**, **JOH**, **LBH**, **KK**, **BR**, **AER**, **KR**, **DS-T**, **AS** and **OT**: writing– original draft (supporting).

Funding This research received no specific grant from any funding agency in the public, commercial, or not-for-profit sectors.

Data availability Most of the observations and interpretations in this paper are derived from integration of published work and inhouse work by Equinor geoscientists, used by permission. All seismic data quoted and used for illustration are proprietary, but are used by permission indicated in the relevant figures.

References

Aarseth, I., Mjelde, R., Breivik, A.J., Minakov, A., Faleide, J.I., Flueh, E. and Huismans, R.S. 2017. Crustal structure and evolution of the Arctic Caledonides: results from controlled-source seismology. *Tectonophysics*, **718**, 9–24, https://doi.org/10.1016/j.tecto.2017.04.022

Abdullah, W.H., Murchinson, D., Jones, J.M., Telnæs, N. and Gjeldberg, J. 1988. Lower Carboniferous coal depositional environments on Spitsbergen, Svalbard. *Organic Geochemistry*, **13**, 953–964, https://doi.org/10.1016/0146-6380(88)90277-X

Allen, P.A. and Allen, J.R. 2013. *Basin Analysis: Principles and Application to Petroleum Play Assessment*. 3rd edn, John Wiley & Sons.

Bergan, M. and Knarud, R. 1993. Apparent changes in clastic mineralogy of the Triassic–Jurassic succession, Norwegian Barents Sea: possible implications for paleodrainage and subsidence. *Norwegian Petroleum Society Special Publications*, **2**, 481–493.

Bjorøy, M., Vigran, J.O. and Rønningsland, T.M. 1978. *Source Rock Evaluation of Mesozoic Shales from Svalbard*. IKU (Continental Shelf Institute) Open Report 160/1/78.

Braathen, A., Bælum, K., Maher, H.D., Jr. and Buckley, S.J. 2011. Growth of extensional faults and folds during deposition of an evaporite-dominated half-graben basin; the Carboniferous Billefjorden Trough, Svalbard. *Norwegian Journal of Geology*, **91**, 137–160.

Bruce, J.R. and Toomey, D.F. 1993. Late Palaeozoic bioherm occurrences of the Finnmark Shelf, Norwegian Barents Sea: analogues and regional significance. *Norwegian Petroleum Society Special Publications*, **2**, 277–292.

Brunstad, H. and Rønnevik, H.C. 2021. Loppa High Tectono-Sedimentary Element, Barents Sea. *Geological Society, London, Memoirs*, **57**, https://doi.org/10.1144/M57-2020-3

Bugge, T., Elvebakk, G. *et al.* 2002. Shallow stratigraphic drilling applied in hydrocarbon exploration of the Nordkapp Basin, Barents Sea. *Marine and Petroleum Geology*, **19**, 13–37, https://doi.org/10.1016/S0264-8172(01)00051-4

Corfu, F., Polteau, S., Planke, S., Faleide, J.I., Svensen, H., Zayoncheck, A. and Stolbov, N. 2013. U–Pb geochronology of Cretaceous magmatism on Svalbard and Franz Josef Land, Barents Sea Large Igneous Province. *Geological Magazine*, **150**, 1127–1135, https://doi.org/10.1017/S0016756813000162

Dalland, A., Worsley, D. and Ofstad, K. (eds). 1988. *A Lithostratigraphic Scheme for the Mesozoic and Cenozoic succession Offshore Mid- and Northern Norway*. Norwegian Petroleum Directorate Bulletin, **4**.

Dallmann, W.K. (ed.) 1999. *Lithostratigraphic Lexicon of Svalbard: Upper Paleozoic to Quaternary Bedrock. Review and Recommendation for Nomenclature Use*. Norwegian Polar Institute, Tromsø, Norway.

Dibner, V.D. (ed.). 1998. *Geology of Franz Josef Land*. Norsk Polarinstitutt Meddelelser, **146**.

Doré, A.G., Corcoran, D.V. and Scotchman, I.C. 2002. Prediction of the hydrocarbon system in exhumed basins, and application to the NW European margin. *Geological Society, London, Special Publications*, **196**, 401–429, https://doi.org/10.1144/GSL.SP.2002.196.01.21

Doré, A.G., Lundin, E.R., Gibbons, A., Sømme, T.O. and Tørudbakken, B.O. 2015. Transform margins of the Arctic: a synthesis and re-evaluation. *Geological Society, London, Special Publications*, **431**, 63–94, https://doi.org/10.1144/SP431.8

Drachev, S.S., Henriksen, E., Sobolev, P. and Shkarubo, S.M. 2021. East Barents Sea Composite Tectono-Sedimentary Element. *Geological Society, London, Memoirs*, **57**, https://doi.org/10.1144/M57-??????

Ebbing, J., Braitenberg, C. and Wienecke, S. 2007. Insights into the lithospheric structure and tectonic setting of the Barents Sea region from isostatic considerations. *Geophysical Journal International*, **171**, 1390–1403, https://doi.org/10.1111/j.1365-246X.2007.03602.x

Eide, C.E., Klausen, T.G., Katkov, D., Suslova, A.A. and Helland-Hansen, W. 2017. Linking an Early Triassic delta to antecedent topography: source-to-sink study of the southwestern Barents Sea margin. *GSA Bulletin*, **130**, 263–283, https://doi.org/10.1130/B31639.1

Faleide, J.I., Bjørlykke, K. and Gabrielsen, R.H. 2010. Geology of the Norwegian Continental Shelf. *In*: Bjørlykke, K. (ed.) *Petroleum Geoscience: From Sedimentary Environments to Rock Physics*. Springer, Berlin. 467–499.

Fleming, E.J., Flowerdew, M.J. *et al*. 2016. Provenance of Triassic sandstones on the southwest Barents Shelf and the implication for sediment dispersal patterns in northwest Pangaea. *Marine and Petroleum Geology*, **78**, 516–535, https://doi.org/10.1016/j.marpetgeo.2016.10.005

Flowerdew, M.J., Fleming, E.J., Morton, A.C., Frei, D., Chew, D.M. and Daly, J.S. 2019. Assessing mineral fertility and bias in sedimentary provenance studies: examples from the Barents Shelf. *Geological Society, London, Special Publications*, **484**, 255–274, https://doi.org/10.1144/SP484.11

Gabrielsen, R.H. and Færseth, R.B. 1989. The inner shelf of North Cape, Norway and its implications for the Barents Shelf–Finnmark Caledonide boundary. A comment. *Norsk Geologisk Tidsskrift*, **69**, 57–62.

Gabrielsen, R.H., Færseth, R.B., Jensen, L.N., Kalheim, J.E. and Riis, F. 1990. *Structural Elements of the Norwegian Continental shelf. Part I: The Barents Sea Region*. Norwegian Petroleum Directorate Bulletin, **6**.

Gee, D.G. and Pease, V. 2004. The Neoproterozoic Timanide Orogen of eastern Baltica: introduction. *Geological Society, London, Memoirs*, **30**, 1–3, https://doi.org/10.1144/GSL.MEM.2004.030.01.01

Gee, D.G. and Teben'kov, A.M. 2004. Svalbard: a fragment of the Laurentian margin. *Geological Society, London, Memoirs*, **30**, 191–206, https://doi.org/10.1144/GSL.MEM.2004.030.01.16

Gernigon, L., Brönner, M., Roberts, D., Olesen, O., Nasuti, A. and Yamasaki, T. 2014. Crustal and basin evolution of the southwestern Barents Sea: from Caledonian orogeny to continental breakup. *Tectonics*, **33**, 347–373, https://doi.org/10.1002/2013TC003439

Glørstad-Clark, E., Birkeland, E.P., Nystuen, J.P., Faleide, J.I. and Midtkandal, I. 2011. Triassic platform-margin deltas in the western Barents Sea. *Marine and Petroleum Geology*, **28**, 1294–1314, https://doi.org/10.1016/j.marpetgeo.2011.03.006

Goutorbe, B., Poort, J., Lucazeau, F. and Raillard, S. 2011. Global heat flow trends resolved from multiple geological and geophysical proxies. *Geophysical Journal International*, **187**, 1405–1419, https://doi.org/10.1111/j.1365-246X.2011.05228.x

Gudlaugsson, S.T. 1993. Large impact crater in the Barents Sea. *Geology*, **21**, 291–294, https://doi.org/10.1130/0091-7613(1993)021<0291:LICITB>2.3.CO;2

Gudlaugsson, S.T., Faleide, J.I., Johansen, S.E. and Breivik, A.J. 1998. Late Palaeozoic structural development of the Southwestern Barents Sea. *Marine and Petroleum Geology*, **12**, 73–102, https://doi.org/10.1016/S0264-8172(97)00048-2

Henriksen, E., Bjørnseth, H.M. *et al*. 2011*a*. Uplift and erosion of the greater Barents Sea: impact on prospectivity and petroleum systems. *Geological Society, London, Memoirs*, **35**, 271–281, https://doi.org/10.1144/M35.17

Henriksen, E., Ryseth, A.E., Larssen, G.B., Heide, T., Rønning, K., Sollid, K. and Stoupakova, A.V. 2011*b*. Tectonostratigraphy of the greater Barents Sea: implications for petroleum systems. *Geological Society, London, Memoirs*, **35**, 163–195, https://doi.org/10.1144/M35.10

Henriksen, E., Ktenas, D. and Nielsen, J.K. 2021*a*. Finnmark Platform Tectono-Sedimentary Element. *Geological Society, London, Memoirs*, **57**, https://doi.org/10.1144/M57-2020-20

Henriksen, E., Kvamme, L. and Rydningen, T.A. 2021*b*. Hammerfest Basin composite Tectono-Sedimentary Element. *Geological Society, London, Memoirs*, **57**, https://doi.org/10.1144/M57-2017-23

Hochuli, P.A. and Feist-Burkhardt, S. 2004. A boreal early cradle of Angiosperms? Angiosperm-like pollen from the Middle Triassic of the Barents Sea (Norway). *Journal of Micropalaeontology*, **23**, 97–104, https://doi.org/10.1144/jm.23.2.97

Hokstad, K., Tašárová, Z.A., Clark, S.A., Kyrkjebø, R., Duffaut, K., Fichler, C. and Wiik, T. 2017. Radiogenic heat production in the crust from inversion of gravity and magnetic data. *Norwegian Journal of Geology*, **97**, 241–254, https://doi.org/10.17850/njg97-3-04

Johansen, S.E., Ostisty, B.K. *et al*. 1993. Hydrocarbon potential in the Barents Sea region: play distribution and potential. *Norwegian Petroleum Society Special Publications*, **2**, 273–320, 1993, https://doi.org/10.1016/B978-0-444-88943-0.50024-1

Kirkland, C.L., Daly, J.S., Eide, E.A. and Whitehouse, M.J. 2006. The structure and timing of lateral escape during the Scandian Orogeny: a combined strain and geochronological investigation in Finnmark, Arctic Norwegian Caledonides. *Tectonophysics*, **425**, 159–189, https://doi.org/10.1016/j.tecto.2006.08.001

Klausen, T.G., Ryseth, A.E., Helland-Hansen, W., Gawthorpe, R. and Laursen, I. 2015. Regional development and sequence stratigraphy of the Middle to Late Triassic Snadd Formation, Norwegian Barents Sea. *Marine and Petroleum Geology*, **62**, 102–122, https://doi.org/10.1016/j.marpetgeo.2015.02.004

Klausen, T.G., Müller, R., Slama, J. and Helland-Hansen, W. 2016. Evidence for Late Triassic provenance areas and Early Jurassic sediment supply turnover in the Barents Sea of northern Pangea. *Lithosphere*, **9**, 14–28, https://doi.org/10.1130/L556.1

Klausen, T.G., Müller, R., Slama, J. and Helland-Hansen, W. 2017*a*. Evidence for late Triassic provenance areas and Early Jurassic sediment supply turnover in the Barents Sea Basin of Northern Pangea. *Lithosphere*, **9**, 14–28, https://doi.org/10.1130/L556.1

Klausen, T.G., Müller, R., Sláma, J., Olaussen, S., Rismyhr, B. and Helland-Hansen, W. 2017*b*. Depositional history of a condensed shallow marine reservoir succession: stratigraphy and detrital zircon geochronology of the Jurassic Stø Formation, Barents Sea. *Journal of the Geological Society, London*, **175**, 130–145, https://doi.org/10.1144/jgs2017-024

Klausen, T.G., Nyberg, B. and Helland-Hansen, W. 2019. The largest delta in Earth's history. *Geology*, **47**, 470–474, https://doi.org/10.1130/G45507.1

Klett, T.R. and Pitman, J.K. 2011. Geology and petroleum potential of the East Barents Sea basins and Admiralty Arch. *Geological Society, London, Memoirs*, **35**, 295–310, https://doi.org/10.1144/M35.19

Klitzke, P., Sippel, J., Faleide, J.I. and Scheck-Wenderoth, M. 2016. A 3D gravity and thermal model for the Barents Sea and Kara Sea. *Tectonophysics*, **684**, 131–147, https://doi.org/10.1016/j.tecto.2016.04.033

Klitzke, P., Faleide, J. I., Scheck-Wenderoth, M., and Sippel, J. 2015. A lithosphere-scale structural model of the Barents Sea and Kara Sea region, Solid Earth, **6**, 153–172, https://doi.org/10.5194/se-6-153-2015

Koehl, J.-B.P., Bergh, S.G., Henningsen, T. and Faleide, J.I. 2018. Middle to Late Devonian–Carboniferous collapse basins on the Finnmark Platform and in the southwesternmost Nordkapp basin, SW Barents Sea. *Solid Earth*, **9**, 341–372, https://doi.org/10.5194/se-9-341-2018

Ktenas, D., Henriksen, E., Meisingset, I., Nielsen, J.K.N. and Andreassen, K. 2017. Quantification of the magnitude of net erosion in the southwest Barents Sea using sonic velocities and compaction trends in shales and sandstones. *Marine and Petroleum Geology*, **88**, 826–844, https://doi.org/10.1016/j.marpetgeo.2017.09.019

Larssen, G.B., Elvebakk, G. *et al*. 2002. *Upper Paleozoic Lithostratigraphy of the Southern Norwegian Barents Sea*. Norwegian Petroleum Directorate Bulletin, **9**.

Lawver, L.A., Grantz, A. and Gahagan, L.M. 2002. Plate kinematic evolution of the present Arctic region since the Ordovician. *Geological Society of America Special Papers*, **360**, 333–358.

Lundschien, B.A., Høy, T. and Mørk, A. 2014. Triassic hydrocarbon potential in the Northern Barents Sea; integrating Svalbard and stratigraphic core data. *Norwegian Petroleum Directorate Bulletin*, **11**, 3–20.

Lundschien, B.A., Mattingsdal, R., Johansen, S.K. and Knutsen, S.M. 2021. North Barents Composite Tectono-Sedimentary Element. *Geological Society, London, Memoirs*, **57**, https://doi.org/10.1144/M57????

McKenzie, D. and Priestley, K. 2016. Speculations on the formation of cratons and cratonic basins. *Earth and Planetary Science Letters*, **435**, 94–104, https://doi.org/10.1016/j.epsl.2015.12.010

Midtkandal, I., Faleide, J.I. *et al*. 2020. Lower Cretaceous Barents Sea strata: Epicontinental basin configuration, timing, correlation and depositional dynamics. *Geological Magazine*, **157**, 458–476, https://doi.org/10.1017/S0016756819000918

Müller, R., Klausen, T.G., Faleide, J.I., Olaussen, S., Eide, C.H. and Suslova, A. 2019. Linking regional unconformities in the Barents Sea to compression-induced forebulge uplift at the Triassic–Jurassic transition. *Tectonophysics*, **765**, 35–51, https://doi.org/10.1016/j.tecto.2019.04.006

NPD. 2018. *Resource Report for Offshore Norway*. Norwegian Petroleum Directorate, Stavanger, Norway, http://www.npd.no/en/Publications/Resource-Reports/2018

NPD. 2019*a*. *Barents Sea Lithostratigraphy*. Norwegian Petroleum Directorate, Stavanger, Norway, https://www.npd.no/facts/geology/lithostratigraphy

NPD. 2019*b*. *Geological Plays*. Norwegian Petroleum Directorate, Stavanger, Norway, http://www.npd.no/en/topics/geology/geological-plays

Nyland, B., Jensen, L.N., Skagen, J., Skarpnes, O. and Vorren, T. 1992. Tertiary Uplift and Erosion in the Barents Sea: magnitude, timing and consequences. *Norwegian Petroleum Society Special Publications*, **1**, 153–162.

Olaussen, S., Larssen, G.B. *et al*. 2018. Mesozoic strata of Kong Karls Land, Svalbard, Norway; a link to the northern Barents Sea basins and platforms. *Norwegian Journal of Geology*, **98**, https://doi.org/10.17850/njg98-4-06

Pascal, C., Balling. N., *et al.* 2010. HeatBar Final Report 2010, Basement heat generation and heat flow in the western Barents Sea – importance for hydrocarbon systems. *Geological Survey of Norway (NGU) Open Report* 2010.030, p.91.

Pastore, Z., Fichler, C. and McEnroe, S.A. 2018. Magnetic anomalies of the mafic/ultramafic Seiland Igneous Province. *Norwegian Journal of Geology*, **98**, 79–101, https://doi.org/10.17850/njg98-1-06

Polteau, S., Hendriks, B.W.H. *et al*. 2016. The Early Cretaceous Barents Sea Sill Complex: distribution, $^{40}Ar/^{39}Ar$ geochronology, and implications for carbon gas formation. *Palaeogeography, Palaeoclimatology, Palaeoecology*, **441**, 83–95, https://doi.org/10.1016/j.palaeo.2015.07.007

Ramberg, I.B., Bryhni, I. and Nøttvedt, A. (eds). 2006. *Landet blir til –Norges geologi*. Norwegian Geological Society, Trondheim, Norway.

Ritzmann, O. and Faleide, J.I. 2009. The crust and mantle lithosphere in the Barents Sea/Kara Sea region. *Tectonophysics*, **470**, 89–104, https://doi.org/10.1016/j.tecto.2008.06.018

Roberts, D. and Siedlecka, A. 2002. Timanian orogenic deformation along the northeastern margin of Baltica, Northwest Russia and Northeast Norway, and Avalonian–Cadomian connections. *Tectonophysics*, **352**, 169–184, https://doi.org/10.1016/S0040-1951(02)00195-6

Ryseth, A. 2014. Sedimentation at the Jurassic–Triassic boundary, south-west Barents Sea: indication of climatic change. *International Association of Sedimentologists Special Publications*, **46**, 187–214.

Ryseth, A.E., Similox-Tohon, D. and Thieβen, O. 2021. Tromsø–Bjørnøya Composite Tectono-Sedimentary Element, Barents Sea. *Geological Society, London, Memoirs*, **57**, https://doi.org/10.1144/M57-2018-19

Shulgin, A., Mjelde, R., Faleide, J.I., Høy, T., Flueh, E. and Thybo, H. 2018. The crustal structure in the transition zone between the western and eastern Barents Sea. *Geophysical Journal International*, **214**, 315–330, https://doi.org/10.1093/gji/ggy139

Slagstad, T., Barrére, C., Davidsen, B. and Ramstad, R.K. 2008. Petrophysical and thermal properties of pre-Devonian basement rocks on the Norwegian continental margin. *Geological Survey of Norway Bulletin*, **448**, 1–6.

Smelror, M., Petrov, O.V., Larssen, G.B. and Werner, S. (eds). 2009. *Geological History of the Barents Sea*. Geological Survey of Norway, Trondheim, Norway.

Sømme, T.O., Doré,, A.G., Lundin, E.R. and Tørudbakken, B.O. 2018. Triassic–Paleogene paleogeography of the Arctic: implications for sediment routing and basin fill. *AAPG Bulletin*, **102**, 2481–2517, https://doi.org/10.1306/05111817254

Stoupakova, A.V., Henriksen, E. *et al*. 2011. The geological evolution and hydrocarbon potential of the Barents and Kara shelves. *Geological Society, London, Memoirs*, **35**, 325–344, https://doi.org/10.1144/M35.21

Suslova, A. 2013. Seismostratigraphic complex of the Jurassic deposits, Barents Sea shelf. *Moscow University Geology Bulletin*, **68**, 68–70, https://doi.org/10.3103/S0145875213030071

Tsikalas, F. 1996. *A Geophysical Study of Mjølnir: A Proposed Impact Structure in the Barents Sea*. PhD thesis, University of Oslo, Oslo, Norway.

Van Koeverden, J.H., Karlsen, D.A., Schwark, L., Chpitsglouz, A. and Backer-Owe, K. 2010. Oil-prone Lower Carboniferous coals in the Norwegian Barents Sea: implications for a Paleozoic petroleum system. *Journal of Petroleum Geology*, **33**, 155–181, https://doi.org/10.1111/j.1747-5457.2010.00471.x

Van Koeverden, J.H., Karlsen, D.A. and Backer-Owe, K. 2011. Carboniferous non-marine source rocks from Spitsbergen and Bjørnøya: comparison with the Western Arctic. *Journal of Petroleum Geology*, **34**, 53–66, https://doi.org/10.1111/j.1747-5457.2011.00493.x

Werner, S. and Torsvik, T.H. 2010. Downsizing the Mjolnir impact structure, Barents Sea, Norway. *Tectonophysics*, **483**, 191–202, https://doi.org/10.1016/j.tecto.2009.08.036

Zhang, X., Pease, V., Carter, A. and Scott, R. 2018. Reconstructing Palaeozoic and Mesozoic tectonic evolution of Novaya Zemlya: combing geochronology and thermochronology. *Geological Society, London, Special Publications*, **460**, 335–353, https://doi.org/10.1144/SP460.13